

I N S T I T U T D ' A E R O N O M I E S P A T I A L E D E B E L G I Q U E

3 - Avenue Circulaire

B - 1180 BRUXELLES

## AERONOMICA ACTA

A - N° 213 - 1980

Stratospheric chemical and thermal response to long-term  
variability in solar UV irradiance

by

G. BRASSEUR and P.C. SIMON

B E L G I S C H I N S T I T U U T V O O R R U I M T E - A E R O N O M I E

3 - Ringlaan

B - 1180 BRUSSEL

## FOREWORD

The paper "Stratospheric chemical and thermal response to long-term variability in solar UV irradiance" is accepted for publication in Journal of Geophysical Research, 86, 1981.

## AVANT-PROPOS

L'article "Stratospheric chemical and thermal response to long-term variability in solar UV irradiance" sera publié dans Journal of Geophysical Research, 86, 1981.

## VOORWOORD

Het artikel "Stratospheric chemical and thermal response to long-term variability in solar UV irradiance" zal verschijnen in Journal of Geophysical Research, 86, 1981.

## VORWORT

Die Arbeit "Stratospheric chemical and thermal response to long-term variability in solar UV irradiance" wird in Journal of Geophysical Research, 86, 1981 herausgegeben werden.

STRATOSPHERIC CHEMICAL AND THERMAL RESPONSE TO LONG-TERM  

---

VARIABILITY IN SOLAR UV IRRADIANCE

---

by

G. BRASSEUR<sup>(\*)</sup> and P.C. SIMON

Institut d'Aéronomie Spatiale  
1180 Brussels - Belgium.

Abstract.

A theoretical analysis of the chemical response of the stratosphere to possible long-term variability of solar ultraviolet irradiance has been performed, taking into account the thermal feedback effect on the reaction rates. Numerical values of ultraviolet and visible irradiation fluxes used in this work are given for aeronomic modeling purposes and a possible variability related to the 11-year solar cycle is suggested on the basis of recent and reliable observations of solar ultraviolet irradiance. This variability has been introduced in a stratospheric two-dimensional model which simulates the zonally averaged distribution of the chemical species related to the oxygen, hydrogen, nitrogen and chlorine families. The results lead to a total ozone variation of the order of 3 percent from the minimum to the maximum solar activity, with a maximum of about ten percent in the upper stratosphere. At these heights, the calculated temperature change is close to 2-4 degrees. The  $N_2O$  concentration appears to be one of the most sensitive to long-term solar variability and a monitoring of this constituent would be useful to give information on the solar variability in the ultraviolet.

---

(\*) Aspirant au Fonds National de la Recherche scientifique.

## Résumé

Une analyse théorique du comportement chimique de la stratosphère aux variations possibles à long terme du rayonnement solaire a été réalisée en tenant compte de l'effet rétroactif des variations en température sur les vitesses de réaction. Des valeurs numériques du flux ultraviolet du soleil sont proposées pour les calculs aéronomiques et une variation avec le cycle de 11 ans est adoptée sur base des observations les plus récentes. Cette variation a été introduite dans un modèle à deux dimensions donnant une distribution moyenne méridionale des constituants oxygénés, hydrogénés, azotés et chlorés. Les résultats du calcul donnent une variation pour le contenu total en ozone de l'ordre de 3% avec le cycle de 11 ans, avec un maximum de l'ordre de 10% dans la stratosphère supérieure où la température varie de 2 à 4 K. La mesure systématique de la concentration en  $N_2O$  qui est très sensible aux variations à long terme du flux ultraviolet solaire pourrait donner une confirmation expérimentale sur celles-ci.

## Samenvatting

Een theoretische analyse van het scheikundig antwoord van de stratosfeer op een mogelijke variatie op lange termijn van de zonnebestralingssterkte werd ondernomen, rekening houdend met het effect van de thermische feedback op de reactiesnelheden. De numerische waarden van de ultraviolet en zichtbare bestralingssterktestroom die in dit werk gebruikt werden zijn voor aeronomische modelisatie doeleinden gegeven en een mogelijke variabiliteit in verband met de 11-jaar zonnecyclus is op basis van recente en betrouwbare waarnemingen van ultraviolet zonnebestralingssterkte voorgesteld. Deze variabiliteit werd gebruikt in een twee-dimensioneel stratosferisch model dat de zonaal gemiddelde distributie van de chemische componenten in verband met zuurstof, waterstof, stikstof en chloraat families simuleert. De resultaten leiden tot een totale ozon variabiliteit van ongeveer 3 percent van de minimum tot de maximum van de zonneactiviteit, met een maximum van ongeveer 10 percent in de hogere stratosfeer. Op deze hoogte is de verandering van berekende temperatuur dicht bij 2-4 graden. De  $N_2O$  dichtheid blijkt een van de meest gevoelige voor de zonnevariabiliteit op lange termijn te zijn en de aanhoudende waarneming van deze component zou zeer nuttig zijn om informatie te geven over de zonnevariabiliteit in het ultraviolet.

## Zusammenfassung

Die chemische Rückwirkungen der Stratosphäre für Variationen der Ultraviolette Strahlung mit thermische Rückwirkung auf die Reaktion Koeffizienten, ist untersucht worden.

Die numerische Werte für die UV und sichtbare Lichtirradiation die in diese Rechnungen genommen sind, wurden in aeronomische Modelle gebraucht. Die eventuelle 11-Jahre Variation der Sonnenaktivität ist von neue und zulässige U-V Beobachtungen abgerechnet worden. Die Variationen sind in einem zwei-dimensionalen Modell mit zonale Mittelwerte der Dichteverteilung für die Molekule die O, H, N und Cl enthalten, berechnet worden. Die Resultaten leiten auf eine gesamte O<sub>3</sub> Variation von ungefähr 3% zwischen das Minimum und das Maximum der Sonnenaktivität. Die grösste Variation (10%) entsteht in der oberen Stratosphäre wo eine Temperaturschwankung von 2-4 K auch resultiert. Die N<sub>2</sub>O Konzentration ist einer der empfänglichsten für langdauer Variationen. Eine kontinuierliche Beobachtung der N<sub>2</sub>O Dichte in der Stratosphäre könnte günstige Informationen über die Variation der Sonnenultraviolette Strahlung geben.

## 1. INTRODUCTION

Studies of the correlation between solar activity and the ozone concentration have a long history. The possibility of such a correlation which was first suggested by Humphreys (1910) has led to much controversy but numerous investigators (Willett, 1962; London and Oltmans, 1973; Paetzold, 1973; Ruderman and Chamerlain, 1975; Angell and Korshover, 1973, 1976), studying the statistics of the ozone data, have quoted a possible relationship between the content of this constituent and the sunspot number. However the observations are controversial because of absolute and intercalibration errors and gaps in data acquisition.

The effects of solar flux variabilities on atmospheric minor constituents have been prior to this work estimated by means of one-dimensional models. Frederick (1977), and Rycroft and Theobald (1978) have studied the chemical response of the upper stratosphere and mesosphere to variations of the solar irradiance with the 27-days solar rotation period. In particular, Frederick (1977) has determined the possible variation in the concentration of mesospheric ozone due to changes in the Lyman  $\alpha$  line intensity. Callis and Nealy (1978a, b), Penner and Chang (1978) and Callis et al. (1979) have estimated the chemical and thermal response of the stratosphere to UV variability associated with the 11-year sunspot cycle adopting various possible solar flux variations among which some are close to irradiance ratio suggested by Heath and Thekaekara (1977). Very recently, Pollack et al. (1979) have investigated the possible climatic impact of UV variations for time scales encompassing the 27 day solar rotation period, the sunspot period, the solar magnetic period and much longer times.

The purpose of this paper is to propose numerical values of UV and visible solar irradiance fluxes in a form which is convenient for

aeronomic modeling purposes. The possible long-term variability of these fluxes will be discussed and a tentative amplitude of these changes versus wavelength will be proposed. The effect of such variability on the chemical and thermal structure of the stratosphere will be examined using a two-dimensional numerical model. In particular, the possible changes in the photodissociation rates of the atmospheric molecules will be studied and the modification of the rate constants due to the temperature variations will be taken into account. Only the flux variability associated with the 11-year cycle will be considered since the change of the solar flux intensity related to the 27-day solar rotation is less than 10 percent above 175 nm (Heath, 1973; Hinteregger *et al.*, 1977) and is of the same order of magnitude as the semi-annual variation in the solar constant ( $\pm 3.3\%$ ) associated with the variation in the Sun-Earth distance.

## 2. THE SOLAR IRRADIATION FLUX AND ITS LONG-TERM VARIABILITY

Recently, Simon (1978, 1979) published a critical review of the available full disk measurements obtained during the solar cycle 20, between 120 and 400 nm, pointing out the disagreements between the most recent data. Since that time, new measurements have been made by Heath (1979), Hinteregger (1980), Mount *et al.* (1980) and Simon *et al.* (1980). Table I gives the most useful observations for aeronomic purposes including date, accuracy and wavelength intervals. In fact, discrepancies of the order of 50 percent still exist for many data, especially in wavelengths particularly important for the photodissociation of molecular oxygen. Consequently, when dealing with atmospheric modeling, a critical study is necessary for the choice of the best solar irradiation flux values.



TABLE 1 : UV solar irradiance measurements relevant for aeronomy

Reference	date of observation	Wavelength interval (nm)	Vehicule	Accuracy
Arvesen <u>et al</u> (1969)	Aug.-Nov. 1967	300-2500	aircraft	$\pm 25 - \pm 3\%$
Ackerman <u>et al</u> (1971)	May 10, 1968			
	Apr. 19, 1969	194-224	balloon	$\pm 20\%$
	Oct. 3, 1969			
Broadfoot (1972)	June 15, 1970	210-320	rocket	$\pm 10\%$
Simon (1974, 1975)	Sept. 23, 1972	196-230	balloon	$\pm 20\%$
	May 16, 1973	285-355		
Rottman (1974)	Dec. 13, 1972	116-185	rocket	$\pm 15\%$
	Aug. 30, 1973			
Samain and Simon (1976)	April 17, 1973	151-209	rocket	$\pm 30\%$
Brueckner <u>et al</u> (1976)	Sept. 4, 1973	174-210	rocket	$\pm 20\%$
Heroux and Swirbalus (1976)	Nov. 2, 1973	123-194	rocket	$\pm 20\%$
Heroux and Hinteregger (1978)	April 23, 1974	25-194	rocket	$\pm 20\%$
Heath (1979)	Nov. 7, 1978	160-400	satellite	$\pm 10 - \pm 3\%$
Simon <u>et al.</u> (1980)	July 1, 1976	210-240	balloon	$\pm 15\%$
	July 7, 1977	275-350		$\pm 10\%$
Hinteregger (1980)	July, 1976 -	15-185	satellite	$\pm 20\%$
	Jan. 22, 1979			
Mount <u>et al.</u> (1980)	June 5, 1979	120-256	rocket	$\pm 15\%$
Simon <u>et al.</u> (1981)	Sept. 14, 1979	210-240	balloon	$\pm 15\%$
	June 24, 1980	275-350		$\pm 10\%$
Neckel and Labs (1981)	1960's	330-1.248	ground	$\pm 1.5 - \pm 1\%$

In the lower thermosphere molecular oxygen is photodissociated by solar irradiation flux ranging from 130 to 175 nm, corresponding to the Schumann-Runge continuum. Only the data of Rottman (1974) Mount et al. (1980), Hinteregger (1980) and Heroux and Swirbalus (1976) cover this entire wavelength range while values of Samain and Simon (1976) and Kjeldseth Moe et al. (1976) begin at 150 and 140 nm respectively. They are not direct full disk irradiance measurements but they were determined from radiance measurements converted into mean intensities using the center-to-limb variation measured by Samain and Simon (1976). The main objective of the observations of Hinteregger (1980) made from the AE-E satellite is to determine the variation of the solar irradiance from 14 to 185 nm. The absolute values are referring to the solar irradiance measurements of April 23, 1974, obtained by means of a rocket experiment (Heroux and Hinteregger, 1978). For these reasons, the rocket measurements performed by Rottman (1974) by Heroux and Swirbalus (1976) and by Mount et al. (1980) seem to us, to be the most reliable observations for aeronomic purposes between 120 and 175 nm. We have chosen Rottman's data obtained on Dec. 13, 1972 to elaborate solar irradiance values averaged over  $500 \text{ cm}^{-1}$  because this observation took place in the middle of the second part of solar cycle 20, and not the value of Mount et al. (1980) which correspond to a maximum of solar activity during the solar cycle 21. A more complete discussion on these data is given by Simon (1981).

Below 90 km photodissociation of molecular oxygen is due to solar radiation ranging from 175 to 240 nm. This process initiates the photochemistry in the mesosphere and in the upper stratosphere. Unfortunately, large discrepancies also exist in the wavelength range mainly between 180 and 190 nm (cf. fig. 6 in Simon, 1978) although rather good agreement exists at 175 nm between Rottman (1974), Heroux and Swirbalus (1976), Brueckner et al. (1976) and Samain and Simon (1976). Only full disk measurements are fully pertinent for aeronomic purposes. Therefore Rottman's values obtained on Dec. 13, 1972 have

been adopted up to 180 nm. Between 180 and 195 nm, it seems appropriate to use an average between the available measurements in order to link Rottman's data with the values of Simon (1974) around 200 nm which have been confirmed by the new observations of Heath (1979). Beyond 210 nm, these latter measurements are lower by a factor varying between 7 and 13 percent than the previous values of Simon (1974) but 27 percent higher than the recent values obtained by Mount et al. (1980) up to 255 nm. A complete discussion on the discrepancies between all these data has been presented by Simon (1981). Consequently, the values of Broadfoot (1972), generally adopted for aeronomic purposes for the wavelengths beyond 230, would be adjusted taking into account the new measurements of Heath (1979), Mount et al. (1980) and Simon et al. (1980). Nevertheless, the lowest data of Mount need to be confirm especially by new rocket observations including solar measurements beyond 255 nm because at longer wavelengths, around 290 nm, both Simon (1975) and Heath (1979) are in very good agreement with Broadfoot (1972).

According to the discussion already published by Simon (1978) on the irradiance data available beyond 290 nm, irradiation flux values obtained by balloon by Simon (1975) have been adopted up to 330 nm. These values are, in addition, in good agreement with the satellite measurement of Heath (1979) and the new balloon observation of Simon et al. (1980). The data of Arvesen et al. (1969) were generally used from 330 nm up to near infrared. Unfortunately the absolute scale used for calibration suffers from uncertainties (Kostkowski, 1974) and it seems preferable to consider the data of Arvesen et al. (1969) as a good relative spectral distribution at medium resolution. The latter values have to be adjusted to the data of Neckel and Labs (1981).

Table II and III give the solar irradiation flux proposed for aeronomic calculations. The values correspond by definition to a mean solar activity and are averaged over several spectral intervals depending on the wavelength range.

TABLE II.1.- Solar irradiation flux  $q$  at one A.U. averaged over  $500 \text{ cm}^{-1}$   
between 117 and 308 nm.

N°	$\Delta\lambda$ (nm)	$\Delta\nu$ ( $\text{cm}^{-1}$ )	$q$ ( $\text{h}\nu \cdot \text{sec}^{-1} \cdot \text{cm}^{-2}$ )
1	Ly $\alpha$ 121.567	82,259	$3.0 \times 10^{11}$
2	116.3-117.0	85,500-86,000	$6.88 \times 10^8$
3	117.0-117.6	85,000-85,500	$2.79 \times 10^9$
4	117.6-118.3	84,500-85,000	$7.30 \times 10^8$
5	118.3-119.0	84,000-84,500	6.51
6	119.0-119.8	83,500-84,000	$1.56 \times 10^9$
7	119.8-120.5	83,000-83,500	1.40
8	120.5-121.2	82,500-83,000	6.30
9	121.2-122.0	82,000-82,500	2.28
10	122.0-122.7	81,500-82,000	1.25
11	122.7-123.5	81,000-81,500	$9.06 \times 10^8$
12	123.5-124.2	80,500-81,000	$1.19 \times 10^9$
13	124.2-125.0	80,000-80,500	$5.95 \times 10^8$
14	125.0-125.8	79,500-80,000	$6.75 \times 10^8$
15	125.8-126.6	79,000-79,500	$1.82 \times 10^9$
16	126.6-127.4	78,500-79,000	$4.56 \times 10^8$
17	127.4-128.2	78,000-78,500	8.01
18	128.2-129.0	77,500-78,000	5.99
19	129.0-129.9	77,000-77,500	7.07
20	129.9-130.7	76,500-77,000	$6.90 \times 10^9$
21	130.7-131.6	76,000-76,500	1.76
22	131.6-132.4	75,500-76,000	$8.24 \times 10^8$
23	132.4-133.3	75,000-75,500	$3.35 \times 10^9$
24	133.3-134.2	74,500-75,000	5.21

TABLE II.1.- (continued)

N°	$\Delta\lambda$ (nm)	$\Delta\nu$ (cm <sup>-1</sup> )	q (hv . sec <sup>-1</sup> . cm <sup>-2</sup> )
25	134.2-135.1	74,000-74,500	8.58 x 10 <sup>8</sup>
26	135.1-136.0	73,500-74,000	2.09 x 10 <sup>9</sup>
27	136.0-137.0	73,000-73,500	1.39
28	137.0-137.9	72,500-73,000	1.18
29	137.9-138.9	72,000-72,500	1.42
30	138.9-140.8	71,000-72,000	6.80
31	140.8-142.8	70,000-71,000	3.81
32	142.8-144.9	69,000-70,000	5.30
33	144.9-147.0	68,000-69,000	7.09
34	147.0-149.2	67,000-68,000	1.10 x 10 <sup>10</sup>
35	149.2-151.5	66,000-67,000	1.22
36	151.5-153.8	65,000-66,000	1.78
37	153.8-156.2	64,000-65,000	2.96
38	156.2-158.7	63,000-64,000	2.41
39	158.7-161.3	62,000-63,000	2.88
40	161.3-163.9	61,000-62,000	3.57
41	163.9-166.7	60,000-61,000	6.07
42	166.7-169.5	59,000-60,000	7.91
43	169.5-172.4	58,000-59,000	1.32 x 10 <sup>11</sup>
44	172.4-173.9	57,500-58,000	7.39 x 10 <sup>10</sup>
45	173.9-175.4	57,000-57,500	8.83
46	175.4-177.0	56,500-57,000	1.13 x 10 <sup>11</sup>
47	177.0-178.6	56,000-56,500	1.35
48	178.6-180.2	55,500-56,000	1.85

TABLE II. 1. - (continued)

N°	$\Delta\lambda(\text{nm})$	$\Delta\nu(\text{cm}^{-1})$	$q(\text{h}\nu \cdot \text{sec}^{-1} \cdot \text{cm}^{-2})$
49	180.2-181.8	55,000-55,500	$1.98 \times 10^{11}$
50	181.8-183.5	54,500-55,000	2.10
51	183.5-185.2	54,000-54,500	1.89
52	185.2-186.9	53,500-54,000	2.90
53	186.9-188.7	53,000-53,500	3.88
54	188.7-190.5	52,500-53,000	4.16
55	190.5-192.3	52,000-52,500	5.60
56	192.3-194.2	51,500-52,000	5.07
57	194.2-196.1	51,000-51,500	7.40
58	196.1-198.0	50,500-51,000	$1.01 \times 10^{12}$
59	198.0-200.0	50,000-50,500	1.20
60	200.0-202.0	49,500-50,000	1.44
61	202.0-204.1	49,000-49,500	1.80
62	204.1-206.2	48,500-49,000	2.08
63	206.2-208.3	48,000-48,500	2.45
64	208.3-210.5	47,500-48,000	5.09
65	210.5-212.8	47,000-47,500	7.12
66	212.8-215.0	46,500-47,000	8.55
67	215.0-217.4	46,000-46,500	9.27
68	217.4-219.8	45,500-46,000	$1.16 \times 10^{13}$
69	219.8-222.2	45,000-45,500	1.20
70	222.2-224.7	44,500-45,000	1.64
71	224.7-227.3	44,000-44,500	1.41
72	227.3-229.9	43,500-44,000	1.46

TABLE II.1.- (continued)

N°	$\Delta\lambda(\text{nm})$	$\Delta\nu(\text{cm}^{-1})$	$q(\text{h}\nu \cdot \text{sec}^{-1} \cdot \text{cm}^{-2})$
73	229.9-232.6	43,000-43,500	$1.68 \times 10^{13}$
74	232.6-235.3	42,500-43,000	1.45
75	235.3-238.1	42,000-42,500	1.74
76	238.1-241.0	41,500-42,000	1.54
77	241.0-243.9	41,000-41,500	2.25
78	243.9-246.9	40,500-41,000	2.05
79	246.9-250.0	40,000-40,500	2.09
80	250.0-253.2	39,500-40,000	2.03
81	253.2-256.4	39,000-39,500	2.96
82	256.4-259.7	38,500-39,000	5.45
83	259.7-263.2	38,000-38,500	4.86
84	263.2-266.7	37,500-38,000	$1.19 \times 10^{14}$
85	266.7-270.3	37,000-37,500	1.29
86	270.3-274.0	36,500-37,000	1.17
87	274.0-277.8	36,000-36,500	1.11
88	277.8-281.7	35,500-36,000	$7.84 \times 10^{13}$
89	281.7-285.7	35,000-35,500	$1.50 \times 10^{14}$
90	285.7-289.9	34,500-35,000	2.12
91	289.9-294.1	34,000-34,500	3.56
92	294.1-298.5	33,500-34,000	3.33
93	298.5-303.0	33,000-33,500	3.08
94	303.0-307.7	32,500-33,000	4.39

TABLE II.2.- Solar irradiation flux  $q$  at one A.U. averaged over 5 nm between 307 and 647 nm.

N°	$\Delta\lambda$ (nm)	$q$ ( $h\nu, \text{sec}^{-1}, \text{cm}^{-2}$ )
95	307.5-312.5	$4.91 \times 10^{14}$
96	312.5-317.5	5.53
97	317.5-322.5	6.04
98	322.5-327.5	6.97
99	327.5-332.5	8.49
100	332.5-337.5	7.52
101	337.5-342.5	8.13
102	342.5-347.5	7.84
103	347.5-352.5	8.31
104	352.5-357.5	9.33
105	357.5-362.5	8.47
106	362.5-367.5	$1.06 \times 10^{15}$
107	367.5-372.5	1.10
108	372.5-377.5	$9.57 \times 10^{14}$
109	377.5-382.5	$1.14 \times 10^{15}$
110	382.5-387.5	$8.63 \times 10^{14}$
111	387.5-392.5	$1.15 \times 10^{15}$
112	392.5-397.5	$9.57 \times 10^{14}$
113	397.5-402.5	$1.70 \times 10^{15}$
114	402.5-407.5	1.70
115	407.5-412.5	1.78
116	412.5-417.5	1.87
117	417.5-422.5	1.84
118	422.5-427.5	1.80



TABLE II.2.- (continued)

N°	$\Delta\lambda$ (nm)	q (hv.sec <sup>-1</sup> .cm <sup>-2</sup> )
119	427.5-432.5	1.66 x 10 <sup>15</sup>
120	432.5-437.5	2.04
121	437.5-442.5	2.00
122	442.5-447.5	2.20
123	447.5-452.5	2.35
124	452.5-457.5	2.30
125	457.5-462.5	2.35
126	462.5-467.5	2.34
127	467.5-472.5	2.36
128	472.5-477.5	2.39
129	477.5-482.5	2.49
130	482.5-487.5	2.30
131	487.5-492.5	2.36
132	492.5-497.5	2.53
133	497.5-502.5	2.38
134	502.5-507.5	2.47
135	507.5-512.5	2.47
136	512.5-517.5	2.32
137	517.5-522.5	2.46
138	522.5-527.5	2.43
139	527.5-532.5	2.60
140	532.5-537.5	2.59
141	537.5-542.5	2.51
142	542.5-547.5	2.56

TABLE II.2.- (continued)

N°	$\Delta\lambda$ (nm)	q (hv.sec <sup>-1</sup> .cm <sup>-2</sup> )
143	547.5-552.5	2.61 x 10 <sup>15</sup>
144	552.5-557.5	2.57
145	557.5-562.5	2.55
146	562.5-567.5	2.61
147	567.5-572.5	2.63
148	572.5-577.5	2.68
149	577.5-582.5	2.66
150	582.5-587.5	2.68
151	587.5-592.5	2.60
152	592.5-597.5	2.67
153	597.5-602.5	2.59
154	602.5-607.5	2.70
155	607.5-612.5	2.64
156	612.5-617.5	2.62
157	617.5-622.5	2.67
158	622.5-627.5	2.62
159	627.5-632.5	2.61
160	632.5-637.5	2.64
161	637.5-642.5	2.62
162	642.5-647.5	2.66

TABLE II.3.- Solar irradiation flux  $q$  at one A.U. averaged over 10 nm  
between 645 and 735 nm.

N°	$\Delta\lambda$ (nm)	$q$ (hv.sec <sup>-1</sup> .cm <sup>-2</sup> )
163	645-655	5.21 x 10 <sup>15</sup>
164	655-665	5.07
165	665-675	5.18
166	675-685	5.15
167	685-695	5.11
168	695-705	5.03
169	705-715	5.00
170	715-725	4.91
171	725-735	4.90

TABLE III.- Solar irradiation flux  $q$  at one A.U. averaged over 1 nm between 116 and 310 nm.

$\Delta\lambda(\text{nm})$	$q(\text{h}\nu \cdot \text{sec}^{-1} \cdot \text{cm}^{-2} \cdot \text{nm}^{-1})$
116 - 117	$9.57 \times 10^8$
117 - 118	$3.34 \times 10^9$
118 - 119	$8.26 \times 10^8$
119 - 120	$2.07 \times 10^9$
120 - 121	6.19
121 - 122	$3.17 \times 10^{12}$
122 - 123	$2.09 \times 10^9$
123 - 124	1.54
124 - 125	1.12
125 - 126	1.17
126 - 127	1.46
127 - 128	$9.71 \times 10^8$
128 - 129	7.50
129 - 130	7.27
130 - 131	$7.29 \times 10^9$
131 - 132	1.31
132 - 133	$9.70 \times 10^8$
133 - 134	$9.40 \times 10^9$
134 - 135	$8.58 \times 10^8$
135 - 136	$2.13 \times 10^9$
136 - 137	1.39
137 - 138	1.33
138 - 139	1.36
139 - 140	3.85
140 - 141	3.27
141 - 142	2.04
142 - 143	2.13

TABLE III.- (continued 1)

$\Delta\lambda(\text{nm})$	$q(\text{h}\nu \cdot \text{sec}^{-1} \cdot \text{cm}^{-2} \cdot \text{nm}^{-1})$
143 - 144	2.60
144 - 145	2.49
145 - 146	2.83
146 - 147	3.81
147 - 148	$4.63 \times 10^9$
148 - 149	4.98
149 - 150	4.74
150 - 151	5.24
151 - 152	5.54
152 - 153	7.40
153 - 154	8.40
154 - 155	$1.36 \times 10^{10}$
155 - 156	1.26
156 - 157	1.19
157 - 158	1.01
158 - 159	$9.50 \times 10^9$
159 - 160	9.78
160 - 161	$1.13 \times 10^{10}$
161 - 162	1.18
162 - 163	1.42
163 - 164	1.65
164 - 165	1.78
165 - 166	2.69
166 - 167	2.10
167 - 168	2.45
168 - 169	3.04
169 - 170	3.89
170 - 171	4.59

TABLE III.- (continued 2)

$\Delta\lambda(\text{nm})$	$q(\text{h}\nu.\text{sec}^{-1}.\text{cm}^{-2}.\text{nm}^{-1})$
171 - 172	4.69
172 - 173	4.96
173 - 174	4.84
174 - 175	5.78
175 - 176	$6.46 \times 10^{10}$
176 - 177	7.00
177 - 178	7.80
178 - 179	8.89
179 - 180	8.74
180 - 181	$1.07 \times 10^{11}$
181 - 182	1.34
182 - 183	1.35
183 - 184	1.35
184 - 185	1.16
185 - 186	1.50
186 - 187	1.83
187 - 188	2.10
188 - 189	2.20
189 - 190	2.35
190 - 191	2.35
191 - 192	3.05
192 - 183	3.16
193 - 194	2.60
194 - 195	4.20
195 - 196	4.05
196 - 197	4.79
197 - 198	5.32

TABLE III.- (continued 3)

$\Delta\lambda(\text{nm})$	$q(\text{hv} \cdot \text{sec}^{-1} \cdot \text{cm}^{-2} \cdot \text{nm}^{-1})$
198 - 199	6.05
199 - 200	5.95
200 - 201	7.11
201 - 202	7.29
202 - 203	8.04
203 - 204	8.93
204 - 205	9.76
205 - 206	9.90
206 - 207	$1.06 \times 10^{12}$
207 - 208	1.20
208 - 209	1.53
209 - 210	2.56
210 - 211	2.92
211 - 212	3.61
212 - 213	3.23
213 - 214	3.43
214 - 215	4.43
215 - 216	4.01
216 - 217	3.73
217 - 218	3.96
218 - 219	4.95
219 - 220	5.27
220 - 221	5.35
221 - 222	4.39
222 - 223	5.68
223 - 224	7.42
224 - 225	6.55
225 - 226	6.13

TABLE III.- (continued 4)

$\Delta\lambda(\text{nm})$	$q(\text{h}\nu \cdot \text{sec}^{-1} \cdot \text{cm}^{-2} \cdot \text{nm}^{-1})$
226 - 227	4.68
227 - 228	4.69
228 - 229	6.22
229 - 230	5.53
230 - 231	6.54
231 - 232	5.83
232 - 233	6.43
233 - 234	5.40
234 - 235	4.65
235 - 236	6.76
236 - 237	5.87
237 - 238	6.38
238 - 239	5.04
239 - 240	5.61
240 - 241	5.22
241 - 242	6.39
242 - 243	8.86
243 - 244	8.03
244 - 245	7.69
245 - 246	6.33
246 - 247	6.40
247 - 248	7.13
248 - 249	5.66
249 - 250	7.35
250 - 251	7.48
251 - 252	5.91
252 - 253	5.60
253 - 254	7.09



TABLE III.- (continued 5)

$\Delta\lambda(\text{nm})$	$q(\text{h}\nu.\text{sec}^{-1}.\text{cm}^{-2}.\text{nm}^{-1})$
254 - 255	$7.80 \times 10^{12}$
255 - 256	$1.14 \times 10^{13}$
256 - 257	1.38
257 - 258	1.68
258 - 259	1.75
259 - 260	1.41
260 - 261	1.34
261 - 262	1.36
262 - 263	1.60
262 - 264	2.33
264 - 265	3.65
265 - 266	3.75
266 - 267	3.50
267 - 268	3.64
268 - 269	3.52
269 - 270	$3.43 \times 10^{13}$
270 - 271	4.00
271 - 272	3.18
272 - 273	2.95
273 - 274	2.81
274 - 275	1.90
275 - 276	2.78
276 - 277	3.60
277 - 278	3.36
278 - 279	2.33
279 - 280	1.26
280 - 281	1.59
281 - 282	3.28

TABLE III.- (end)

$\Delta\lambda(\text{nm})$	$q(\text{h}\nu.\text{sec}^{-1}.\text{cm}^{-2}.\text{nm}^{-1})$
282 - 283	4.37
283 - 284	4.71
284 - 285	3.50
285 - 286	2.03
286 - 287	4.62
287 - 288	5.38
288 - 289	4.46
289 - 290	6.65
290 - 291	9.12
291 - 292	8.82
292 - 293	8.04
293 - 294	8.07
294 - 295	7.56
295 - 296	8.17
296 - 297	7.36
297 - 298	7.97
298 - 299	$6.21 \times 10^{13}$
299 - 300	7.32
300 - 301	6.10
301 - 302	6.77
302 - 303	7.38
303 - 304	9.65
304 - 305	9.37
305 - 306	8.93
306 - 307	8.89
307 - 308	$1.00 \times 10^{14}$
308 - 309	$9.54 \times 10^{13}$
309 - 310	7.55

As long-term variability of UV solar irradiance is quite evident at Lyman  $\alpha$  and below 100 nm (Vidal Madjar, 1975; Schmidtke, 1978), such a variation is expected at longer wavelength with a magnitude which has to be established. Unfortunately, in the wavelength range of stratospheric interest, the evidence of variations during solar cycle 20 is not conclusive as it was stated by Simon (1978) and by Delaboudinière et al. (1978). This is due to the inadequate time coverage of reliable data during the solar cycle 20, to the uncertainties associated with each observation and to the absence of intercomparison in the calibration procedures. Nevertheless, Heath and Thekaekara (1977) claimed an 11-year variability of a factor of 2 at 200 nm on the basis of their own measurements performed by satellites and by rockets since 1966. This is illustrated in fig. 1 on which the full squares and triangles represent the solar flux ratio from minimum to maximum solar activity obtained from broadband photometric observations and the full circles the ratio obtained by means of a double monochromator experiment. The solid curve represents the solar variability deduced by the authors. It should be pointed out that there are only two points around 180 nm and that the solar flux ratios obtained around 290 nm with the double monochromator are 15-20 percent higher than those obtained from the broadband detectors at the same wavelength. In addition, the accuracy of the basic measurements obtained from this latter instrument is  $\pm 15$  percent and  $\pm 30$  percent for the shorter and the longer wavelength respectively and between  $\pm 8$  percent and  $\pm 3$  percent for the double monochromator data. A linear regression calculation is shown by the dashed lines for each set of solar flux ratios. Extrapolation of solar flux ratio at 340 nm from the broadband detector measurements gives a variability of 25 percent between irradiances corresponding to the maximum and to the minimum of the 11-year solar cycle. Such a value is in contradiction with the variability based on the double monochromator data. On the other hand, extrapolation of the latter data to shorter wavelength gives a ratio of only 0.7 at 200 nm. If variations with the 11-year cycle in the ultraviolet solar irradiance do exist, they are probably less than those stated by Heath and Thekaekara (1977).

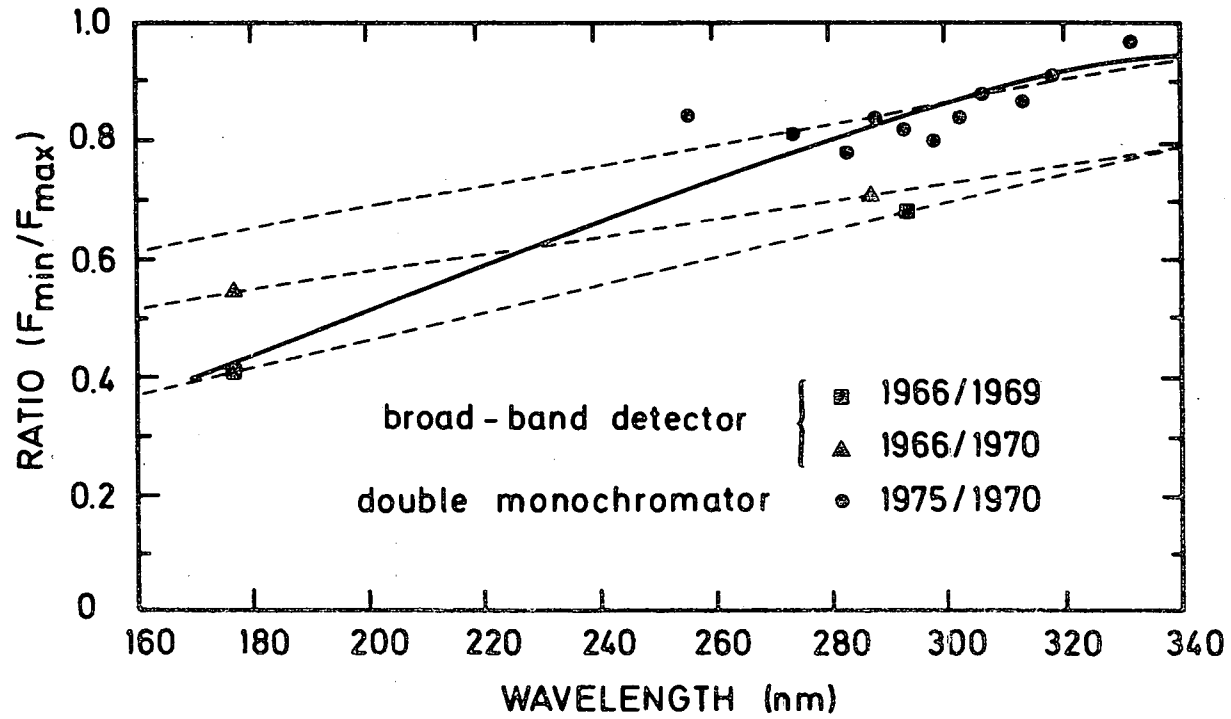


Fig. 1.- Ratio of solar flux measured near solar-cycle minimum to that measured near solar-cycle maximum versus wavelength claimed by Heath and Thekaekara (1977). (Solid line). The full squares and triangles are based on broadband photometric observations and the full circles on a double monochromator experiment.

Such a comment seems to be confirmed by Hinteregger (1980) for observations performed between 1976 and 1979 for wavelengths below 185 nm, leading to a variability of 21% around 180 nm during that time and by new observations performed by balloon in 1976 and 1977 (Simon et al. 1980) corresponding to the minimum solar activity between solar cycle 20 and 21. Variations between 210 and 240 nm over the 11-year cycle may not exceed 20 percent if differences between observations are interpreted only as variations of the solar output and not as experimental errors.

The previous considerations lead us to adopt a solar irradiance ratio between the minimum and the maximum of the 11-year cycle varying from 0.8 at 200 nm to 0 at 300 nm. These ratios are illustrated in fig. 2 and have been introduced in our calculations.

### 3. THEORETICAL RESPONSE OF THE STRATOSPHERE TO UV VARIABILITY ASSOCIATED WITH THE 11-YEAR SUNSPOT CYCLE

Using a two-dimensional model of the stratosphere which has been described in several previous papers (Brasseur, 1976; 1978; Brasseur and Bertin, 1976; 1978), we have studied the relationship between the solar variability and the stratospheric minor constituents at various latitudes. The model has been used with steady state conditions since the run of the time dependent version for a period of 2 or 3 solar cycles consumes a prohibitive amount of computer time. A thermal scheme has been added to the chemical approach in order to take into account the thermal feedback in the chemical responses. The distribution in the meridional plane of the following species is calculated :  $O_3$ ,  $O(^3P)$ ,  $O(^1D)$ , OH,  $HO_2$ ,  $N_2O$ , NO,  $NO_2$ ,  $N_2O_5$ ,  $HNO_3$ ,  $CH_4$ ,  $CH_3Cl$ ,  $CFCl_3$ ,  $CF_2Cl_2$ ,  $CCl_4$ , Cl, ClO,  $ClONO_2$ , HCl. The water vapor is being held constant; since  $H_2O$  appears to be less sensitive to the photochemistry than to the transport, this hypothesis should not seriously alter our conclusions.

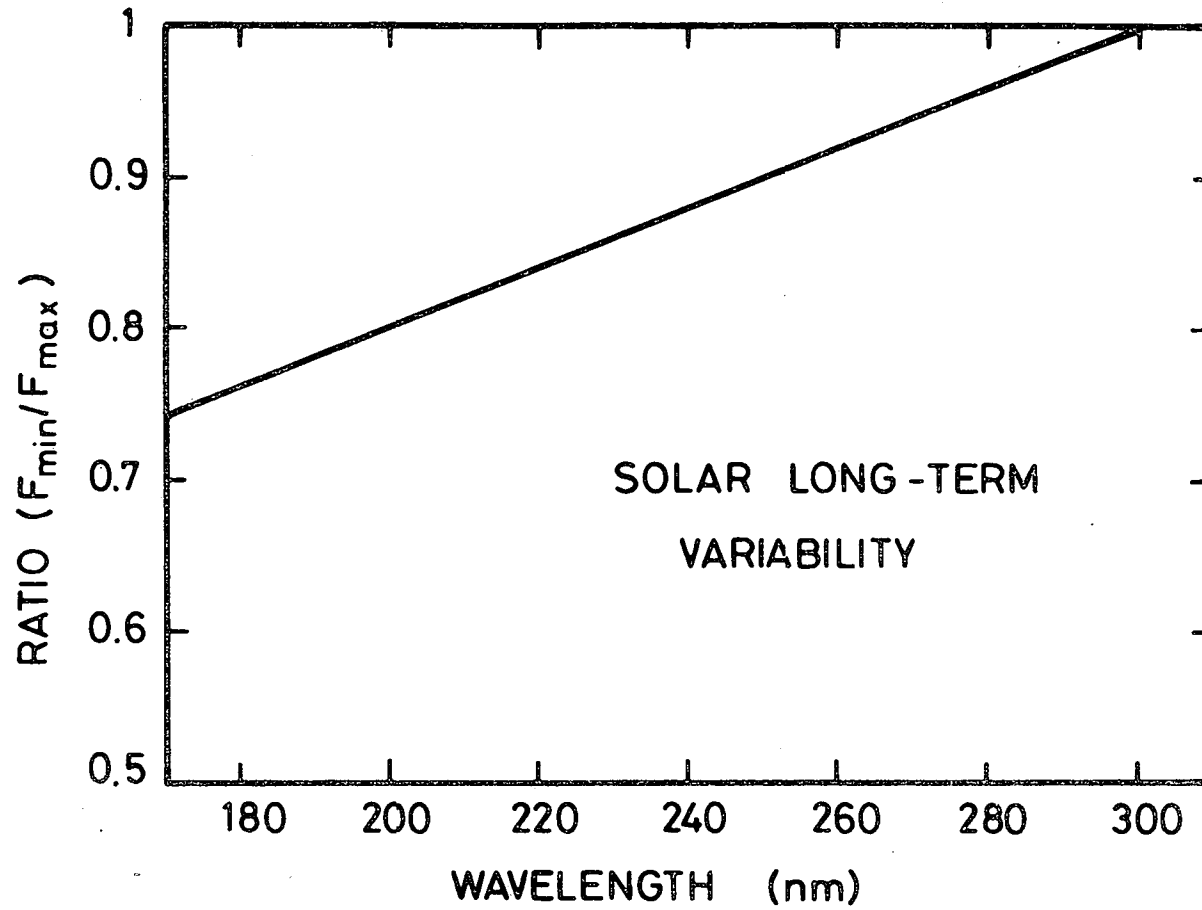


Fig. 2.- Long-term solar variability adopted in this work. The curve representing the ratio between minimum and maximum irradiance refers to an upper limit of variability during the 11-year sunspot cycle.

The steady state assumption needs further justification since species with long chemical lifetime ( $N_2O$ ,  $CH_4$ ,  $CFCI_3$ ,  $CF_2Cl_2$ , etc..) may be expected to respond with a certain delay which is not negligible compared with 11 years. In fact, the variability of minor constituents appears with the highest efficiency in the regions where the photochemistry is the most active, that is where the lifetime of the species is the shortest. As shown by Callis and Nealy (1978) and by Penner and Chang (1978), in their 1-D models, the time lag for long lived species such as  $N_2O$  is significant only in the altitude range where the magnitude of the variation is very small. The calculated ozone change by these authors using a full interactive time dependent calculation, is thus nearly identical to that obtained with a steady state model.

On the other hand, there may be significant differences between steady and time-dependent calculations for more reactive species such as  $HNO_3$ ,  $H_2O_2$  and  $ClONO_2$  leading in steady state models to errors in the calculations of both local and total ozone. Again, this effect and the possible significant phase difference with respect to solar activity appears essentially in the lower stratosphere where the relative ozone variation is the smallest. Nevertheless further investigation should estimate the impact of seasonal variations in the calculations, particularly in a two-dimensional representation.

In order to determine the concentration of constituents (or family of constituents such as  $NO_y$  ( $= NO + NO_2 + HNO_3 + ClONO_2$ ) or  $CIX$  ( $= Cl + ClO + HCl + ClONO_2$ )) we have solved for each of them a continuity equation. The meridional distribution of the temperature  $T$  is obtained by solving the equation of energy conservation.

A detailed description of the model with the related numerical method and the physical and chemical conditions is given in the appendix.

#### 4. ANALYSIS OF THE RESULTS

---

The model has been run for three different scenarios. In the first case, a solar flux  $q_{\text{mean}}$  corresponding to average irradiance conditions is adopted; the second and third cases refer respectively to high ( $q_{\text{max}}$ ) and low ( $q_{\text{min}}$ ) solar activity. The fractional variation of a quantity  $X$ , expressed in percent, is then defined as :

$$\frac{\Delta X}{X} = \frac{X(q_{\text{max}}) - X(q_{\text{min}})}{X(q_{\text{mean}})} \times 100$$

The temperature variation however is expressed by its absolute value

$$\Delta T = T(q_{\text{max}}) - T(q_{\text{min}})$$

The primary effect of the solar flux variation as shown by figure 2 appears through a change in the photodissociation rates for the molecules absorbing below 300 nm. Figure 3 shows the relative variation of photodissociation frequencies for various stratospheric species. Due to larger variations of ultraviolet flux around 200 nm, compounds absorbing mainly in the shorter wavelengths range are obviously more sensitive than constituents whose absorption peaks are observed in the visible or in the near UV. For example, when the solar irradiance increases from the minimum to the maximum, the production rate of ozone related to the dissociation of  $O_2$  increases more significantly than the dissociation of  $O_3$ .

The second chemical response appears through the change in the temperature distribution since chemical reaction rates are generally temperature dependent. This effect is not negligible as shown by the following example which refers to simplified conditions. If a pure oxygen atmosphere is assumed, the ozone concentration above 25-30 km is given by (Nicolet, 1971)

$$n(O_3) = [J n(M) n^2(O_2) K]^{1/2}$$



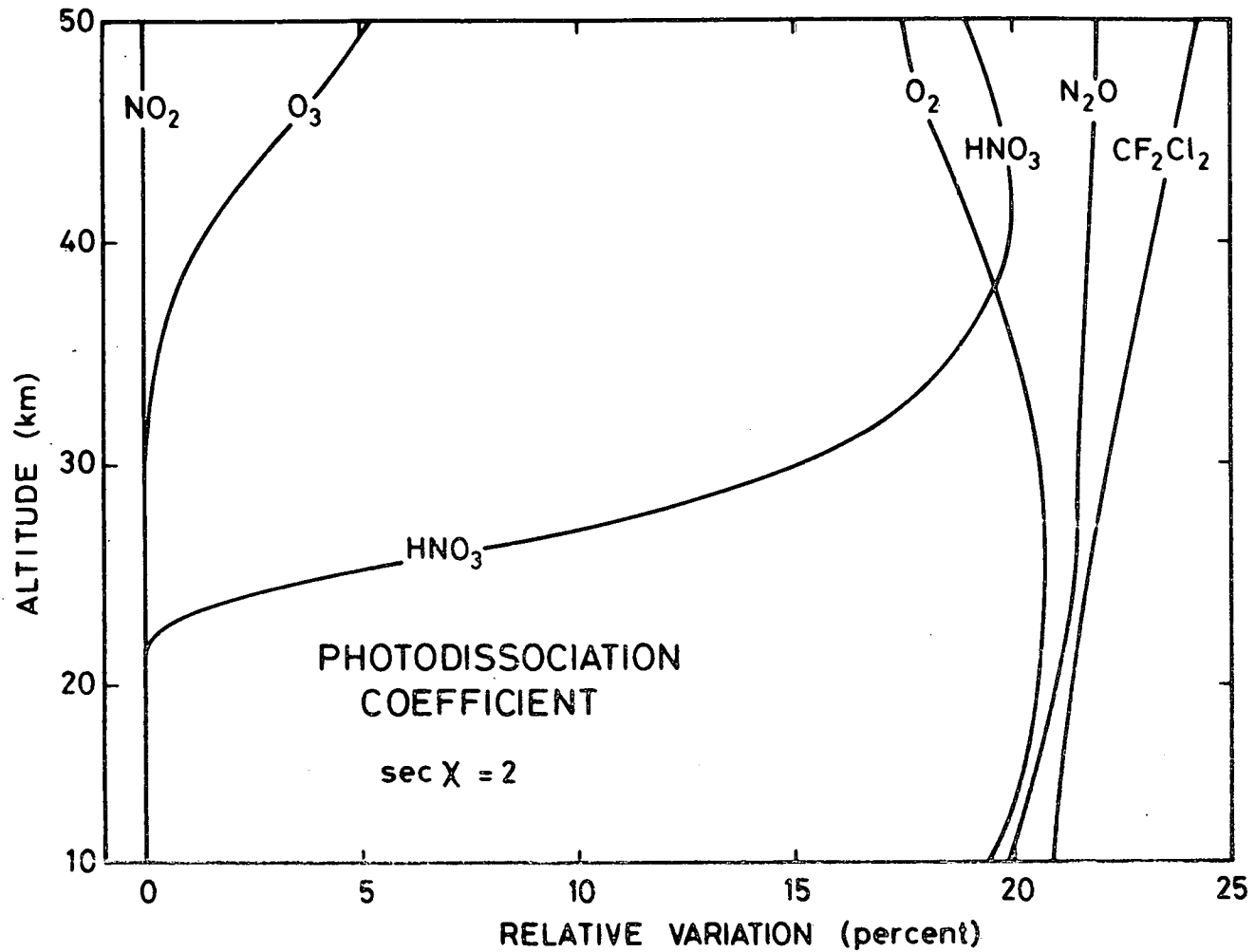


Fig. 3.- Relative variation of the photodissociation frequency of various stratospheric species as a function of the altitude and for a solar zenith angle of 60 degrees.

where  $K = k_2/k_3$  (see table III) and where  $J = J_{O_2}/J_{O_3}$  is the ratio of the  $O_2$  and  $O_3$  photodissociation rates. The fractional variation in the ozone concentration can be written, if the molecular oxygen and total concentrations are assumed to remain unchanged,

$$\frac{\Delta n(O_3)}{n(O_3)} \approx \frac{1}{2} \frac{\Delta J}{J} + \frac{1}{2} \frac{\Delta K}{K}$$

The first term, which is the direct effect via the photodissociation rates, is positive (fig. 4) since  $\Delta J_{O_2}/J_{O_2} > \Delta J_{O_3}/J_{O_3}$ . The second term which represents the indirect effect via the temperature change is negative since  $\Delta K/K \cong -2810 \Delta T/T^2$ . In fact, the temperature dependence of the recombination rate of O and  $O_3$  (reaction  $k_3$ , see table 3) reduces the variation of the ozone concentration as computed when the temperature feedback is omitted. In the real atmosphere, the problem is more complex since the interaction with other constituents ( $HO_x$ ,  $NO_x$ , CIX, etc...) has to be taken into consideration and the full model calculation has to be performed. However, the temperature effect appears mainly through the direct recombination of O and  $O_3$ .

A third effect, which is not included in this work, could play a certain role, namely the variation of the total concentration which, according to the hydrostatic law, should be associated with any temperature change. This variation could affect the three body reaction rates (see for example reactions  $k_2$ ,  $a_1$ , etc..., table IV in the appendix and the concentration of minor constituents above 35-40 km (Penner and Luther, 1980).

Figure 5 depicts the percent change in ozone concentration from solar minimum to solar maximum, as computed in the 2-D model using the full chemistry of table IV (see appendix). Curve (a) represents the vertical distribution of  $O_3$  at 30 degrees latitude when the temperature feedback is taken into account. In curve (b) the temperature is held

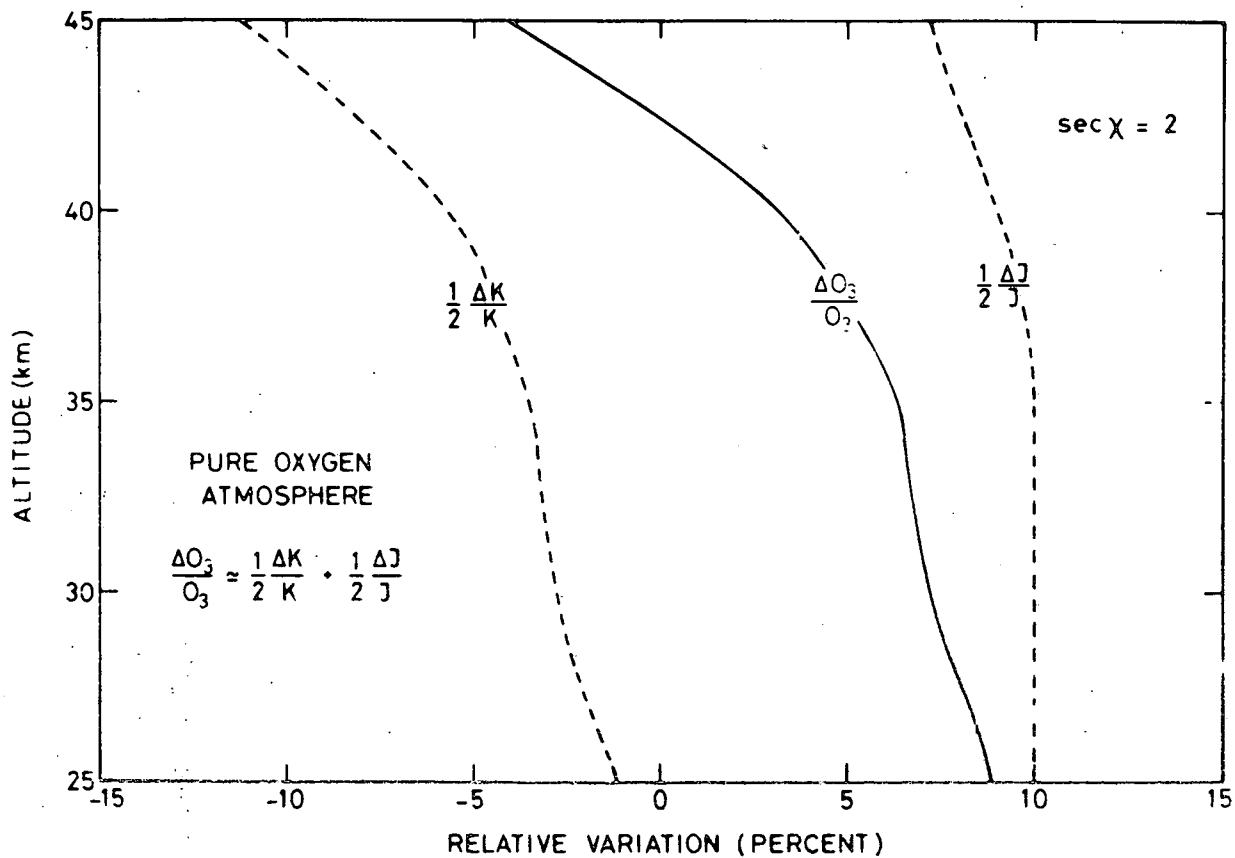


**Fig. 4.-** Relative variation of the ozone concentration versus altitude in a pure oxygen atmosphere for a zenith angle of 60 degrees. The curve labelled  $\Delta J/2J$  refers to the contribution of the change in the photodissociation rates while the curve labelled  $\Delta K/2K$  represents the effect of the following temperature variations :  $\Delta T = 0.4$  K at 25 km, 1.1 at 30 km, 1.6 at 35 km, 3.0 at 40 km and 6.0 at 45 km.

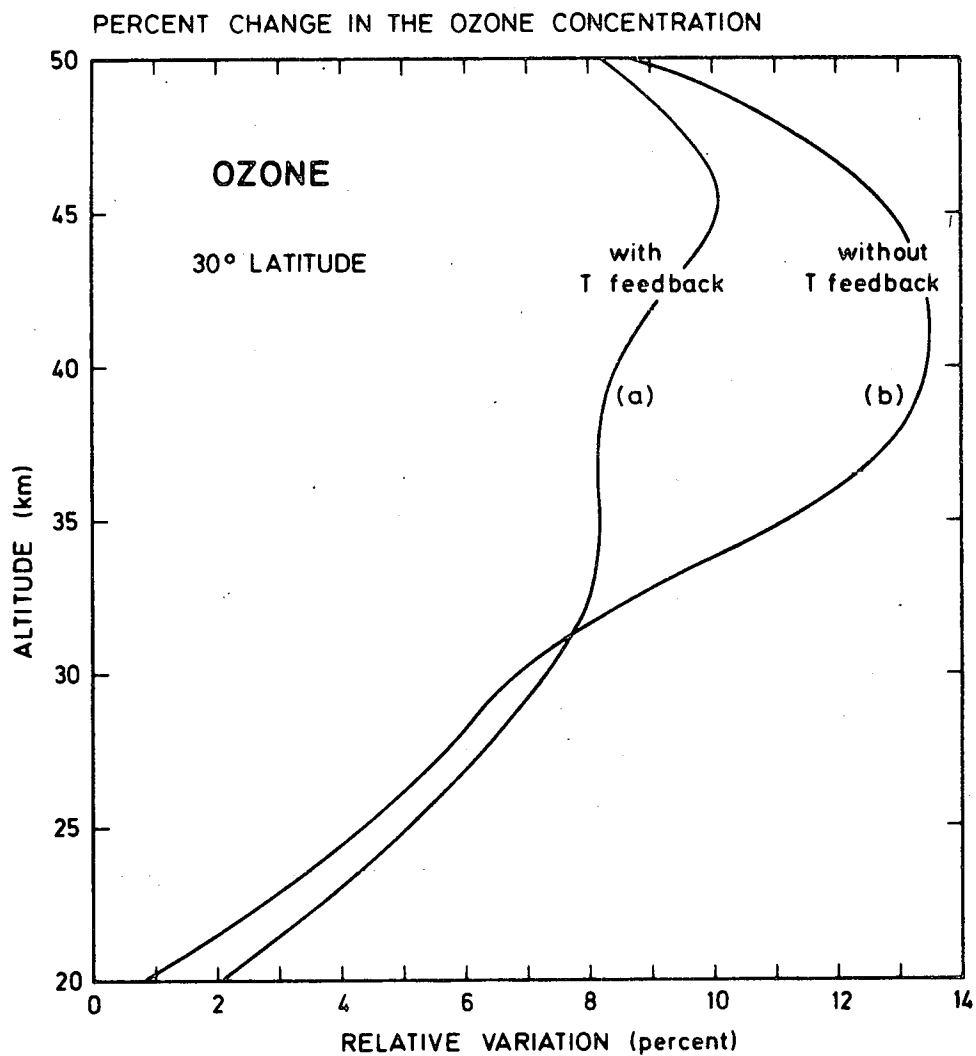


Fig. 5.- Relative change of the ozone concentration versus altitude at 30 degrees latitude (yearly mean) related to the solar irradiance variation as indicated in fig. 2. Curve (a) with temperature feedback. Curve (b) with fixed temperature.

constant. In this latter case, the ozone concentration increases with the solar flux, the maximum variation (13 percent) appearing around 40 km. This large increase of  $O_3$  in the upper stratosphere is due to the enhanced dissociation rate of molecular oxygen in this altitude range. Moreover, in the vicinity of the stratopause (and in the lower mesosphere), the enhancement of  $O_3$  becomes smaller due to the increase of the OH and  $HO_2$  concentration. In the lower stratosphere, the increase of  $O_3$  is relatively small since the penetration of UV radiation in the Herzberg continuum is reduced by the enhancement of the ozone content at higher altitude and by the fact that  $O_3$  becomes less sensitive to chemistry and photochemistry. In order to illustrate this point, fig. 6 depicts the variation of the average ozone production rate at 35 and 20 km respectively. In the upper stratosphere of the equatorial regions, the photodissociation rate of  $O_2$  leading to the formation of  $O_3$  is increased by more than 10 percent from solar minimum to solar maximum. But in the lower stratosphere, due to the enhancement of the optical depth above this level, the production rate of ozone is reduced by a factor which increases with latitude (i.e. with optical depth or solar zenith angle). At 20 km this reduction varies from about 2 percent at the equator to 10 percent at 60 degrees latitude. The loss rate of  $O_3$  is also modified. It increases with solar flux in the upper stratosphere so that a new photochemical equilibrium is reached with a corresponding value of the ozone concentration. In the lower stratosphere, the loss rate decreases with increasing solar irradiance but the new ozone concentration depends on the transport conditions which are kept unchanged in the present model.

When the temperature feedback is considered, the ozone variation as given by the model calculation, is reduced above 30 km and the maximum (10 percent) raises to about 45 km. This reduction is explained by the negative correlation between  $O_3$  and temperature. Below 30 km, in the region where the peak of the ozone concentration is located, the ozone enhancement is slightly larger when the temperature

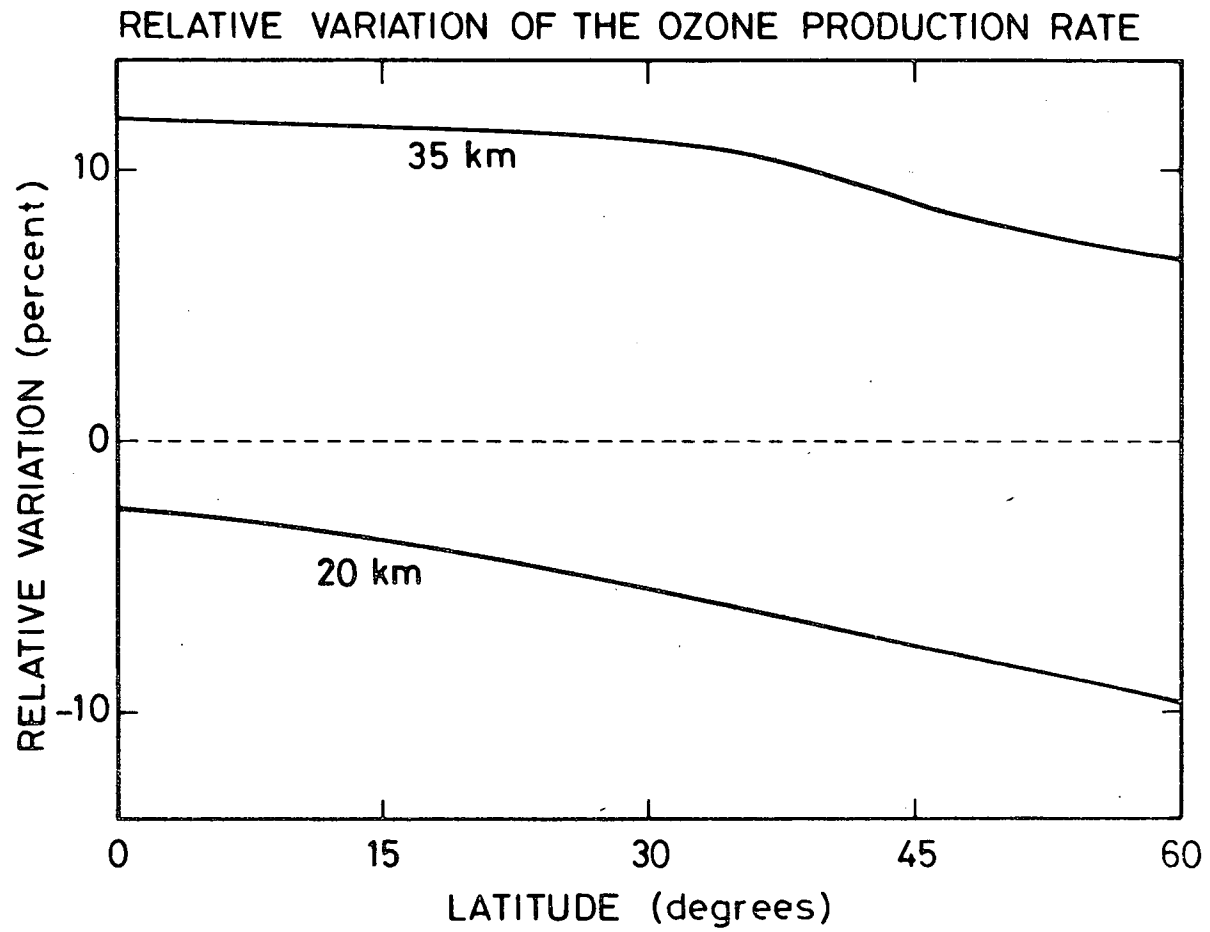


Fig. 6.- Relative variation of the ozone production rate as a function of the latitude at 20 and 35 km respectively.

feedback is considered. Again this is related to the variation of ozone at higher altitude and the penetration of UV radiation down to the lower stratosphere. With the spectral distribution of the solar variability adopted in this paper, the relative change of the ozone column has the same order of magnitude (3 percent) in both cases (with and without temperature feedback). Moreover, as stated by fig. 7, the total ozone variation  $\Delta O_3/O_3$  does not show any appreciable latitudinal variation if the proposed solar variability is used in the model calculation. In fact, as shown in fig. 8, the equatorial regions are characterized by a relatively large ozone enhancement at high altitudes and a small variation at low altitudes, while at higher latitudes the ozone variation is relatively constant between 20 and 45 km. This effect can be explained by the feedback between the vertical ozone distribution and the penetration of the UV radiation responsible for the ozone formation.

Fig. 9 shows, for comparison purposes, the ozone variations at  $30^\circ$  latitude due to the flux variability adopted in this work and those due to higher variability proposed by Heath and Thekaekara (1977). The magnitude of the  $O_3$  variation is enhanced from 10 to 22 percent at 45 km. Since this last number is much larger than the observed changes of the ozone concentration in the upper stratosphere (Angell and Korshover, 1978a), the solar flux variability given by Heath and Thekaekara (1977) is probably largely overestimated. When the latter solar variability is introduced in the model calculation, the increase in the total ozone concentration shows a more pronounced latitudinal variation (fig. 7). This effect can be explained by the fact that, in this latter case, the solar irradiance is modified as far as 350 nm, i.e. in a region where ozone is photodissociated and molecular oxygen is not. Therefore, the variation of the  $J_{O_2}/J_{O_3}$  ratio is more sensitive to the solar zenith angle in the case of the Heath and Thekaekara model than in the case of the solar flux variability as suggested in this paper.

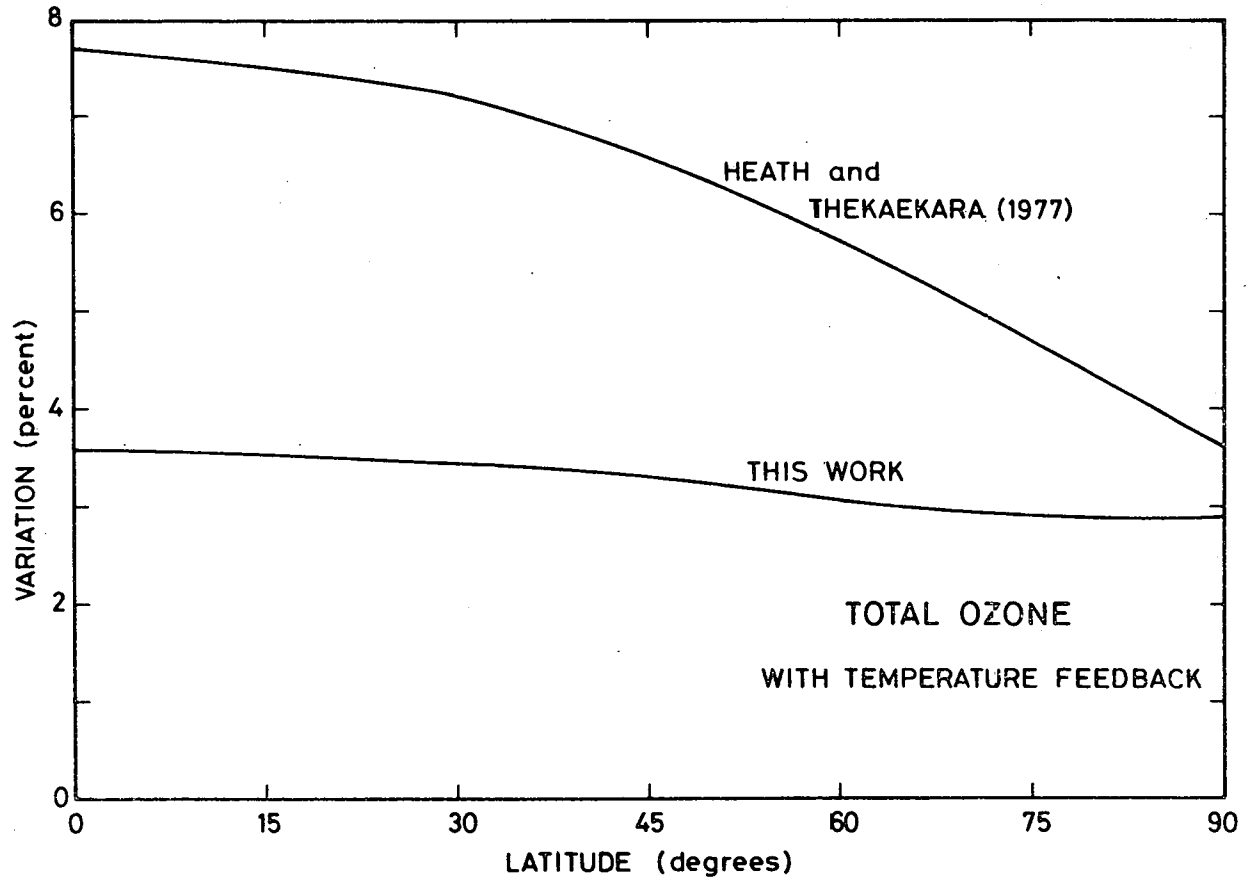


Fig. 7.- Relative variation of the vertically integrated ozone concentration as a function of the latitude assuming two different solar flux variabilities (fig. 1 - solid line and fig. 2)



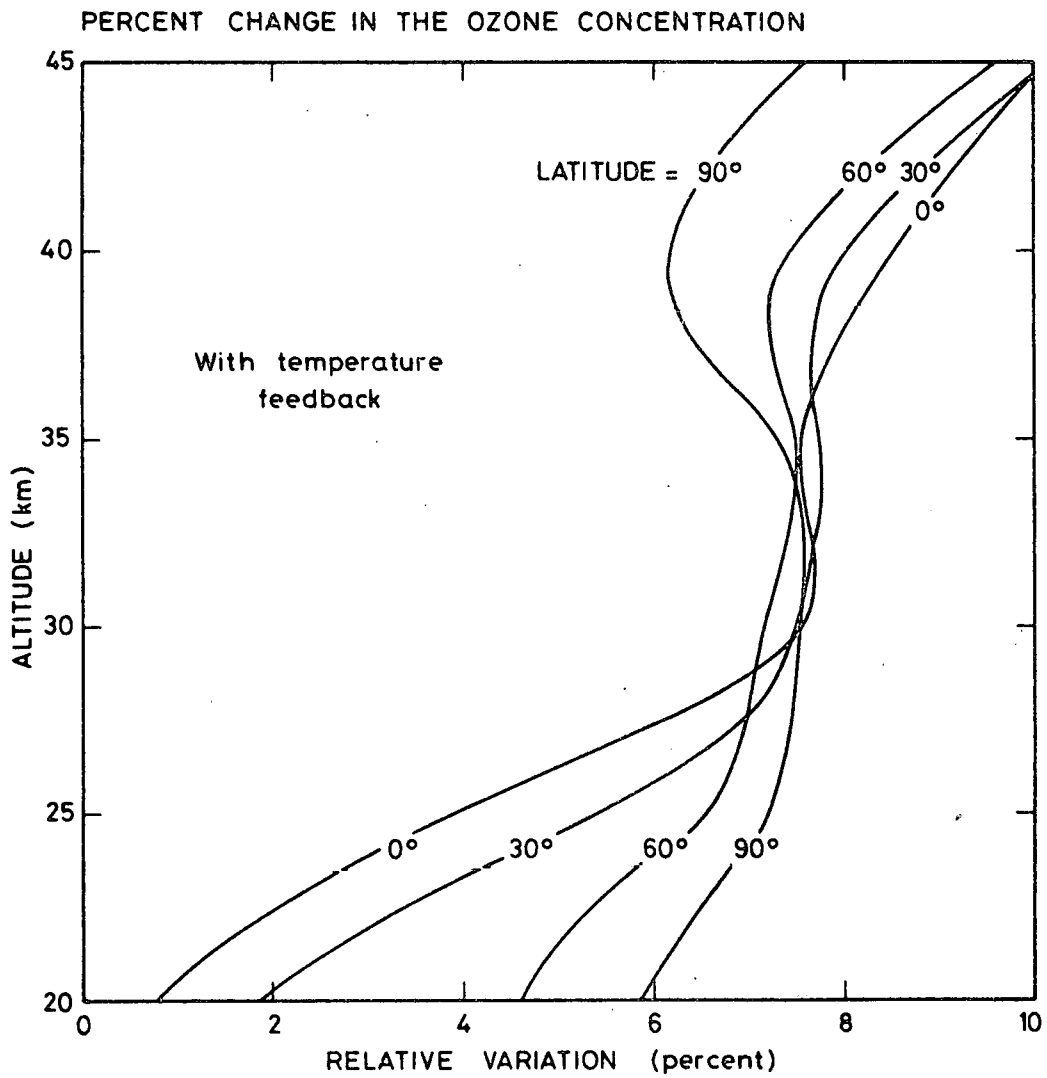


Fig. 8.- Relative variation of the ozone concentration versus altitude at different latitudes in response to the UV variability from solar minimum to maximum (fig. 2).

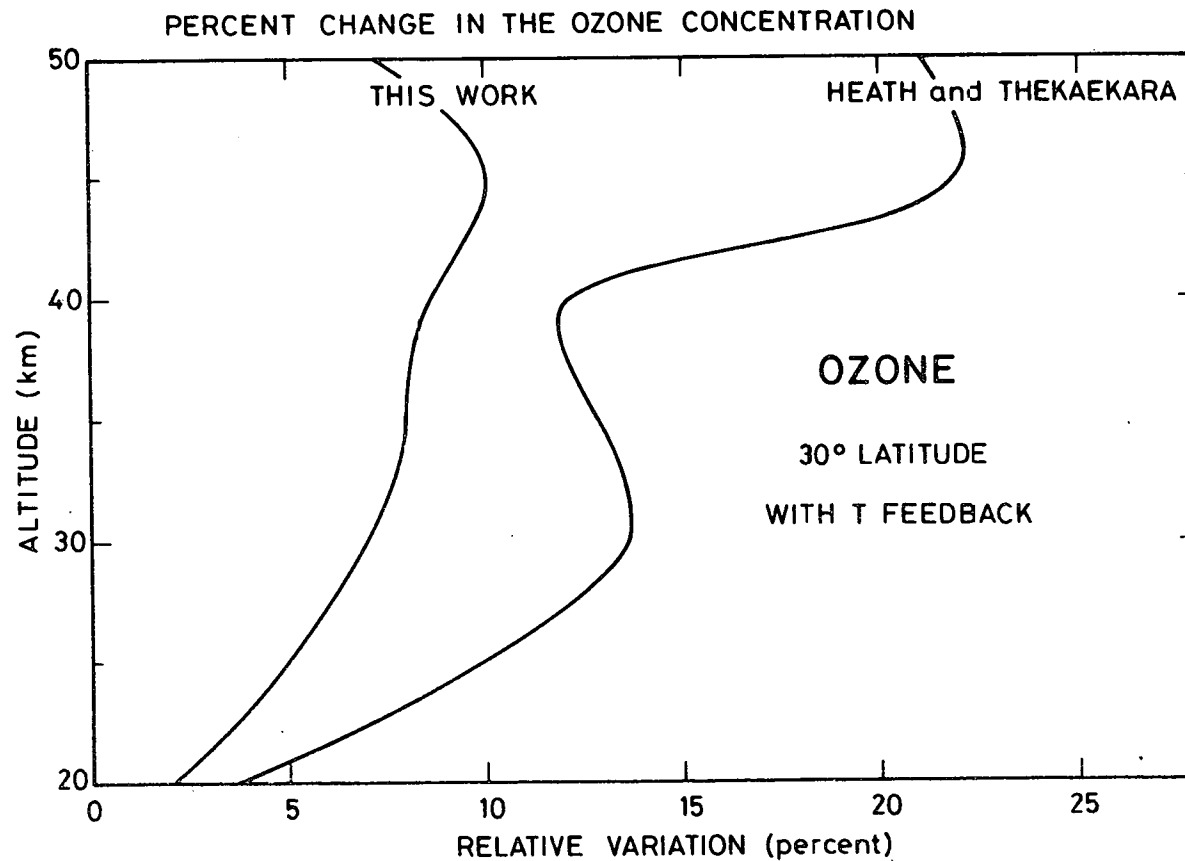


Fig. 9.- Relative variation of the ozone concentration versus altitude for two different solar flux variabilities (see fig. 1 - solid line and fig. 2).

The numbers obtained in the present computation are not inconsistent with the analysis of the ozone data by Angell and Korshover (1978a). These show in the Northern Hemisphere where most stations are located a 5 percent increase in total ozone between the early 60's and 70's and a 1-2 percent decrease between 1970 and 72. The analysis of Angell and Korshover (1978a) also indicates that the Umkehr data in the North temperate latitudes suggest a 11 percent increase of the ozone concentration in the 32-46 km layer between 1964 and 1970.

On the other hand, calculations of the possible modulation of stratospheric ozone due to the penetration variability in the atmospheric of galactic cosmic rays (Ruderman and Chamberlain, 1975) and the related formation of nitrogen oxides in the lower stratosphere, mainly at high latitude (Warneck, 1972; Nicolet and Peetermans, 1972; Brasseur and Nicolet, 1973; Nicolet, 1975), have been performed. Our model shows that this effect can be neglected in comparison with the ozone modulation due to UV variability as adopted in this work.

Finally the corresponding changes in the heating rate by  $O_3$  absorption and in the temperature distribution as determined by our 2-D model are shown respectively in fig. 10 and 11. The temperature increases with solar flux mainly above 30 km because of the enhanced ozone heating by UV fluxes. The effect which is most significant in the equatorial and tropical regions must be related to the meridional distribution of the ozone variation (fig. 9). A comparison with the results obtained by Callis and Nealy (1978) and, to a certain extent, by Penner and Chang (1978) indicate that the temperature variation values obtained by these authors are significantly larger than ours.

It should also be noted that Callis and Nealy (1978b) have derived a negative variation of the ozone concentration in the upper stratosphere while the results obtained by Callis and Nealy (1978a), by Penner and Chang (1978) and by ourselves show a positive variation.

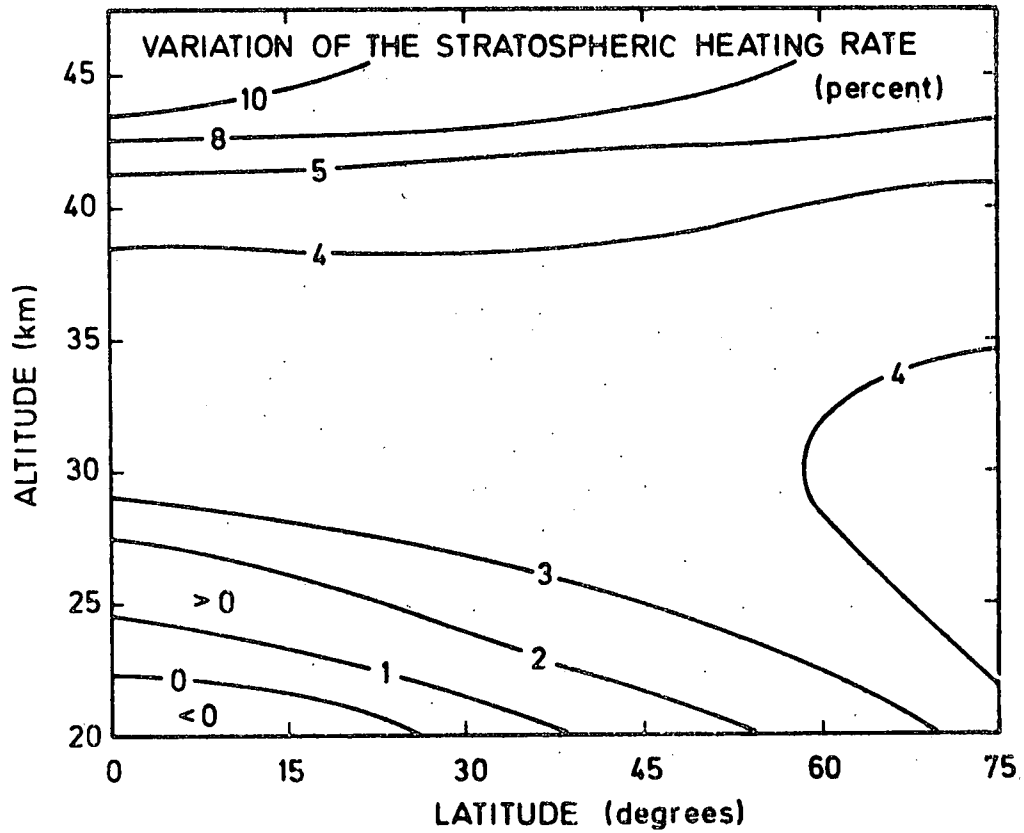


Fig. 10.- Meridional distribution of the relative variation in the heating rate for the UV variability from solar minimum to maximum (fig. 2).

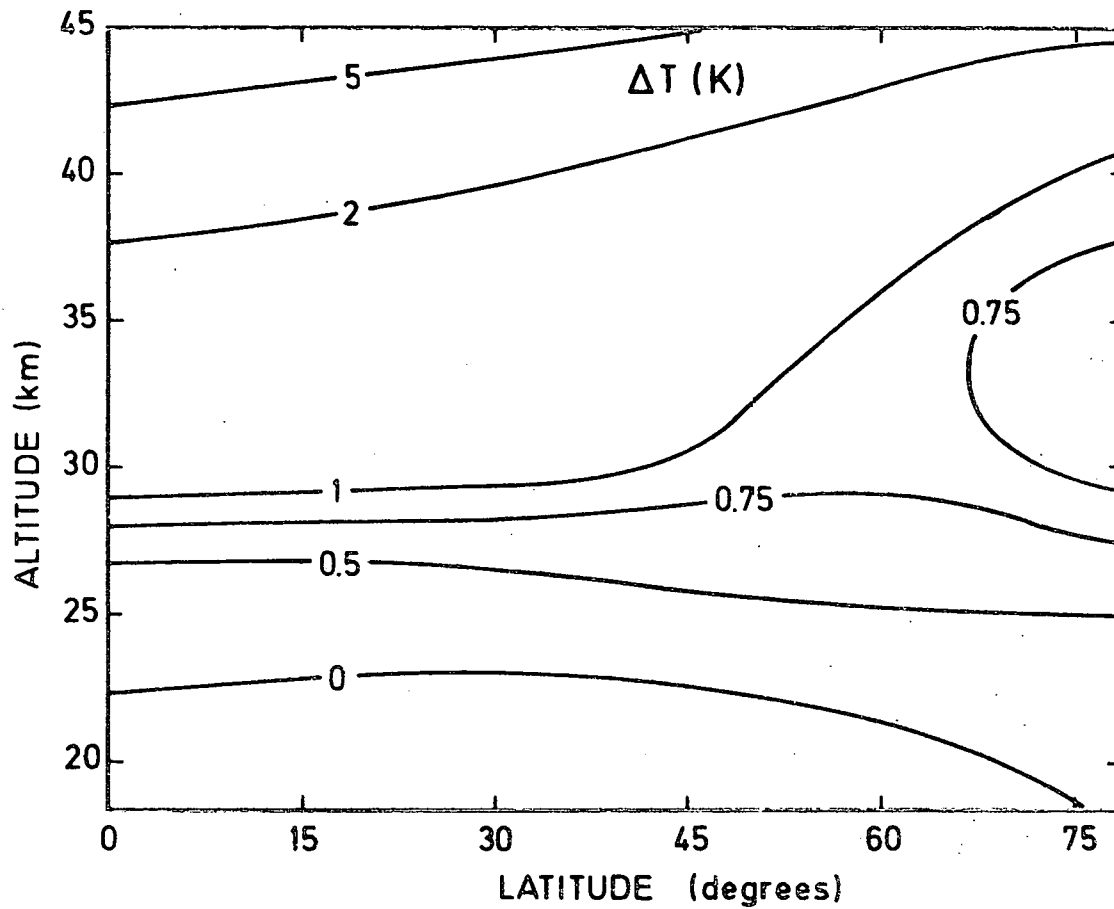


Fig. 11.- Meridional distribution of the relative change in the temperature for the UV variability from solar minimum to maximum (fig. 2).

The difference may be mainly due to the magnitude of the temperature change which as mentioned is much larger in the results of Callis and Nealy (1978b).

The stratospheric temperature trends observed since the 1960's have been analyzed by different authors (Angell and Korshover, 1978b; Quiroz, 1979). The warming occurring prior to 1970 in the middle and upper stratosphere and the cooling recorded in the beginning of the 1970's shows a high correlation with solar cycle 20 as quoted by Quiroz (1979). This author has indicated that the corresponding temperature change from solar maximum (1969) to solar minimum (1975) varies among the stations from  $-3^{\circ}\text{C}$  to  $-6^{\circ}\text{C}$  in the upper stratosphere. These values are in fairly good agreement with our results at 45 km which provide a variation of  $6^{\circ}\text{C}$  at the equator and  $3^{\circ}\text{C}$  at 60 degrees. However, below 40 km, the computed temperature change seems smaller than the observations. Moreover, the variations reported by Quiroz (1979) appears to be fairly uniform among most stations while our results show some latitudinal variations.

The effect of the UV variability on atomic oxygen is illustrated in fig. 12. The enhancement at high altitude of the concentration associated with a higher solar flux value is due, for  $\text{O}(^3\text{P})$  and  $\text{O}(^1\text{D})$ , to the increased concentration of ozone and to the increased rate of its photodissociation. In the lower stratosphere, the negative change of the  $\text{O}(^1\text{D})$  concentration is due to the increased absorption of UV radiation by ozone, the concentration of which becomes larger at higher altitudes.

The percentage change of the hydroxyl and hydroperoxyl radicals concentration is represented in fig. 13. This graph shows a global increase with altitude of the  $\text{HO}_x$  variation, which can be explained by a similar increase of the  $\text{O}(^1\text{D})$  variation with height. The presence of OH and  $\text{HO}_2$  radicals in the stratosphere is primarily due to the oxidation of water vapor, methane and molecular hydrogen by  $\text{O}(^1\text{D})$

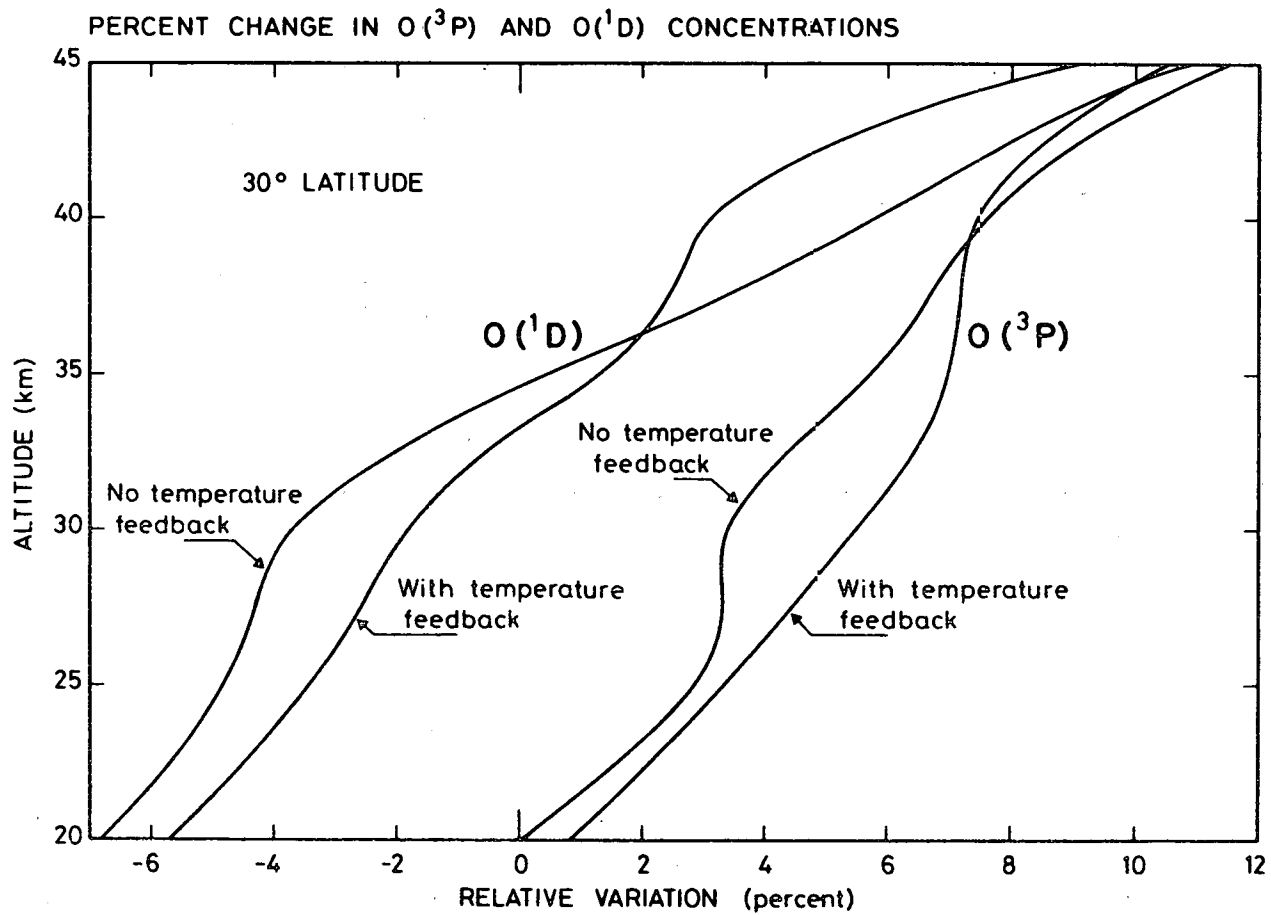


Fig. 12.- Vertical distribution of the relative change in the average atomic oxygen concentration at 30 degrees latitude for the UV variability from solar minimum to maximum (fig. 2).

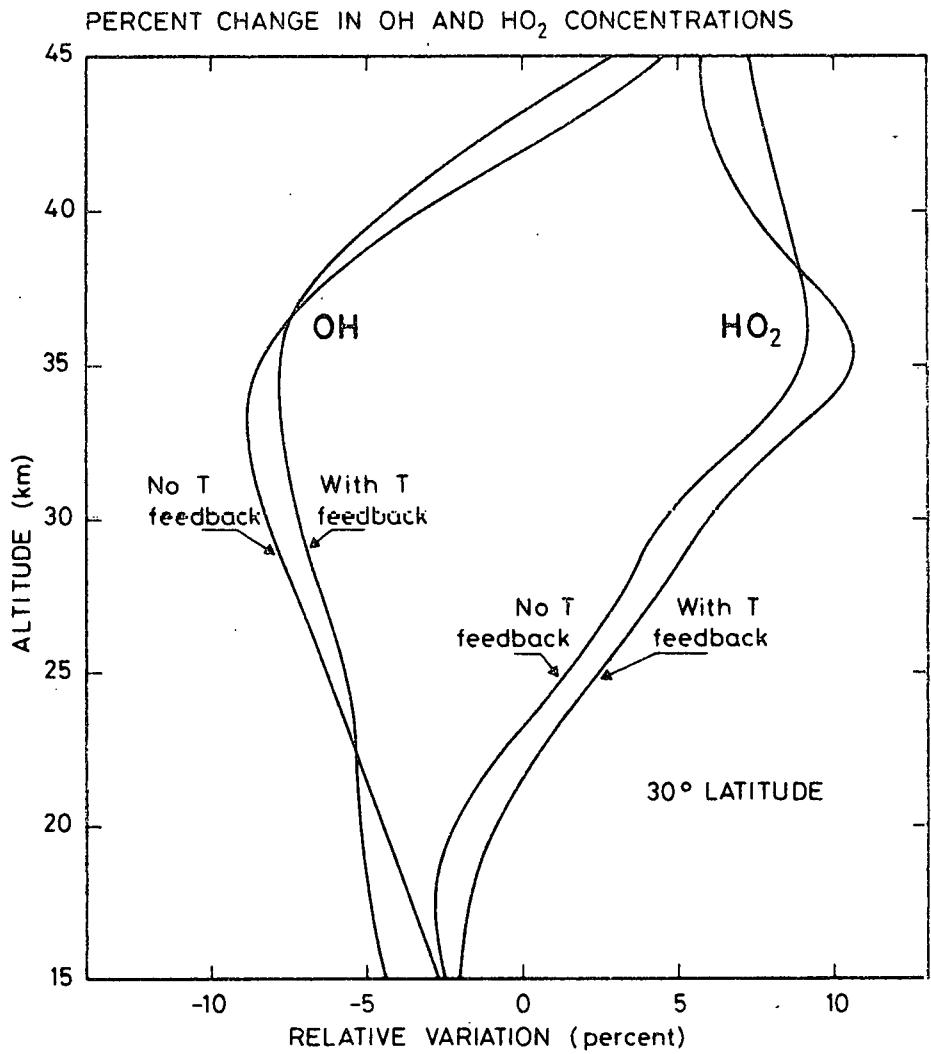


Fig. 13.- Vertical distribution of the relative change in the average hydroxyl and hydroperoxyl radicals concentration at 30 degrees latitude for the UV variability from solar minimum to maximum (fig. 2).



atoms. As stated above, the water vapor is held constant in the model. However had water vapor been allowed to vary, there would have been a small increase of  $H_2O$  (Penner and Chang, 1980) due to more oxidation of methane. This should lead to an increase of the OH and  $HO_2$  concentration in the upper stratosphere and consequently for OH to a lower crossover point from negative to positive variations. These changes should have a limited impact on the ClO/HCl concentration ratio but the effect on ozone is not expected to be large.

The change in the  $HO_2$  to OH ratio, which also appears, is related to the variation of  $O_3$ ,  $O(^3P)$ , NO and CO which determines the value of this ratio. Near the stratopause, one can see that the factor  $n(HO_2)/n(OH)$  remains unchanged since it becomes almost independent of any concentration.

The relative variation of long lived species produced at ground level such as  $N_2O$ ,  $CCl_4$ ,  $CFCl_3$  and  $CF_2Cl_2$  is illustrated in figure 14 and 15 assuming for these constituents a fixed concentration at ground level and steady state conditions. In both cases, large perturbations are obtained but these occur at high altitude where the concentration becomes relatively small. Nevertheless, the long term measurement of the concentration of such species around 40 km should give an indication of the real existence of a solar variability associated with the 11-year cycle. For  $N_2O$ ,  $CCl_4$ ,  $CFCl_3$  and  $CF_2Cl_2$ , the negative variation computed in the model is due to the increase in the photodissociation rate of these molecules. However, the production rate of ClX which is the product of the dissociation coefficient and the concentration of halocarbons (varying with opposite signs) varies locally much less and its integrated value remains unchanged if the flux at ground level is kept constant (atmospheric release of chlorofluorocarbons). Moreover it should be noted that  $CH_3Cl$ , the most important producer of ClX in the natural stratosphere, is positively correlated with the UV flux since its main destruction is due to the reaction with

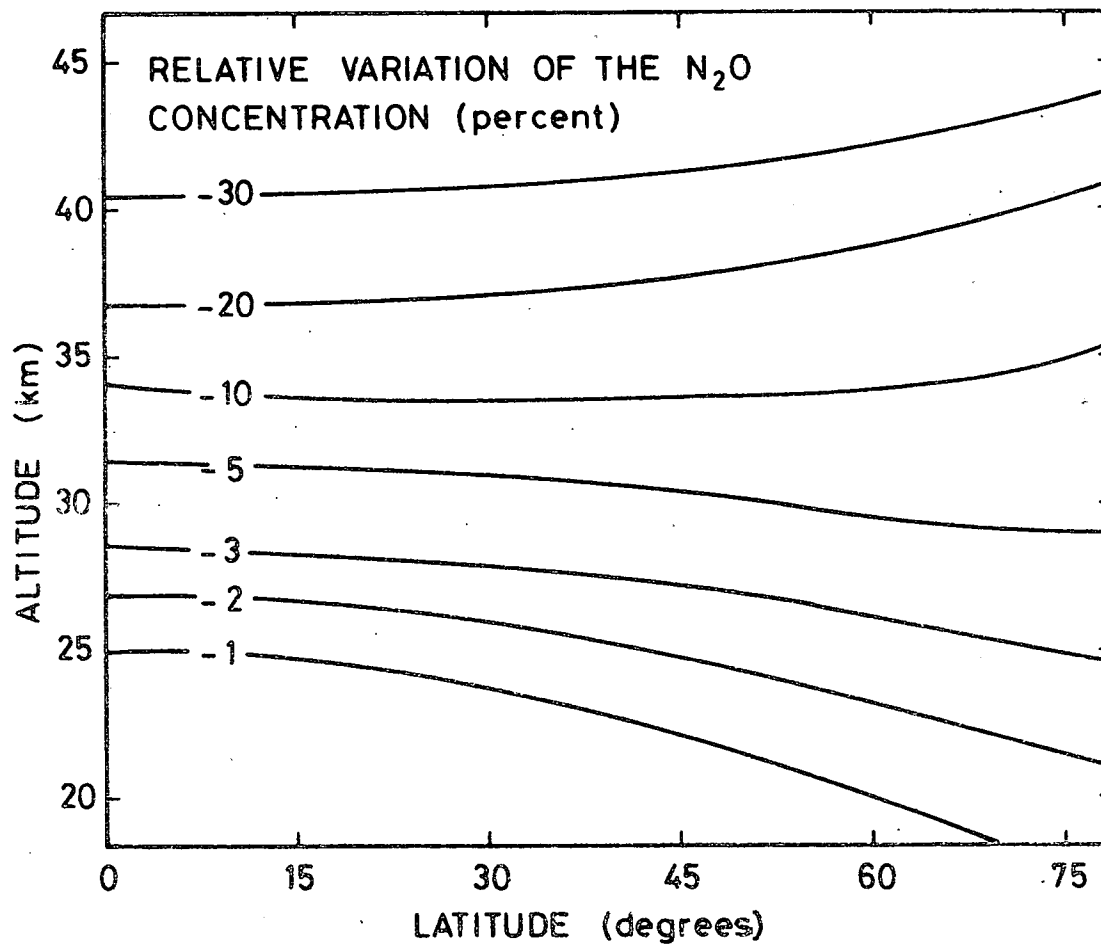


Fig. 14.- Meridional distribution of the relative change in the nitrous oxide concentration for the UV variability as represented in fig. 2. Temperature feedback taken into account.

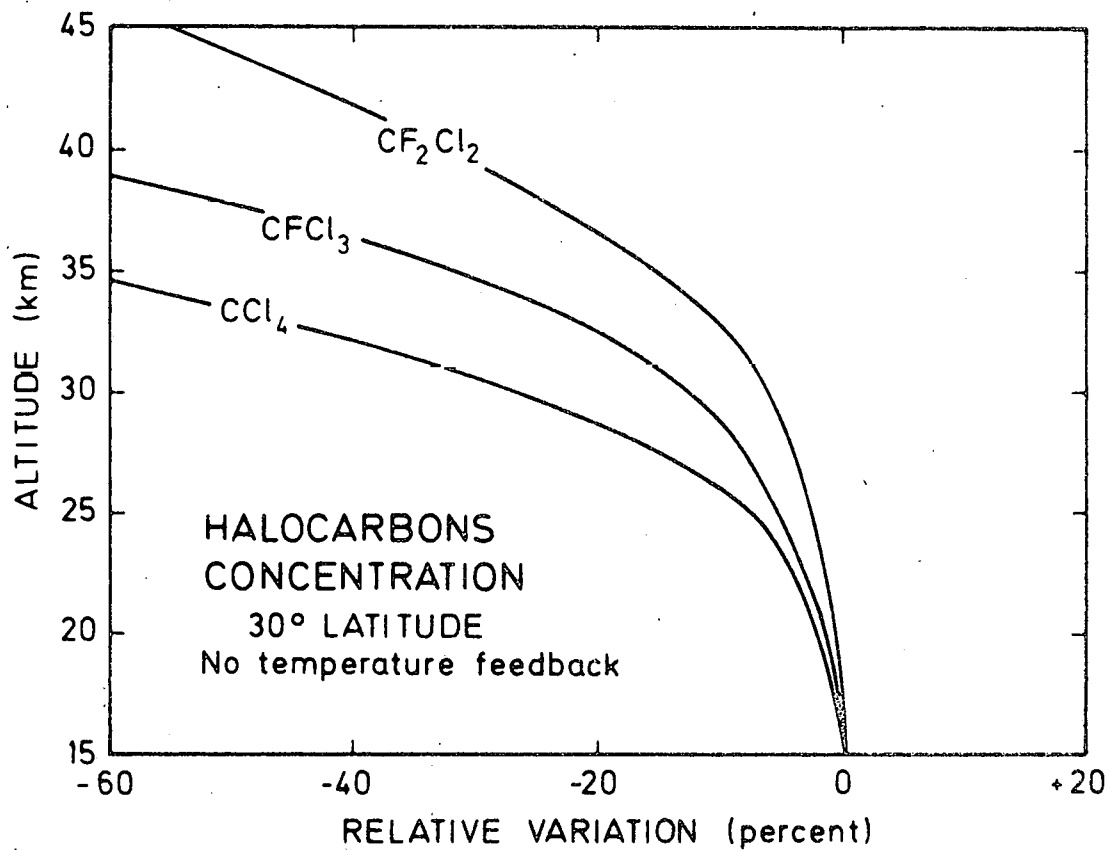


Fig. 15.- Vertical distribution at 30 degrees latitude of the relative change in the concentration of  $CCl_4$ ,  $CFCl_3$  and  $CF_2Cl_2$  from solar minimum to maximum (fig. 2).

hydroxyl radicals OH which are slightly depleted when the solar irradiance increases. The same effect appears for methane. The calculations referring to ClO and HCl indicate that the average concentration varies in both cases by less than 4 percent.

Odd nitrogen in the stratosphere is formed by the reaction between  $N_2O$  and  $O(^1D)$ . The variation in the corresponding production rate, illustrated in figure 16, is negative and yields 30 percent above 44 km in the equatorial region. Therefore, the decrease of the  $NO_x$  concentration (figure 17) can be significant mainly in the upper stratosphere and should contribute to increase the ozone concentration in this region.

## 5. CONCLUDING REMARKS

There are indications that the UV irradiance responsible for the photodissociation of several minor constituents and for the local heating in the stratosphere, shows time variations related to the 11-year solar cycle. However the variability suggested by Heath and Thekaekara (1977) seems to be overestimated if a critical analysis of the solar irradiance measurements is performed. Therefore a more realistic dependence on wavelength, based on several observations including recent balloon measurements, is suggested.

If such a variation is applied to the stratospheric photochemical and thermal calculations, a total ozone variation of the order of 3 percent from the minimum to the maximum solar activity should be expected. The largest change, namely 10 percent when the temperature feedback is taken into account, appears in the upper stratosphere. The corresponding calculations with the solar flux variability of Heath and Thekaekara (1977) lead to ozone variations (24 percent at 45 km and 30 degrees) which should be detected with the current ozone network.

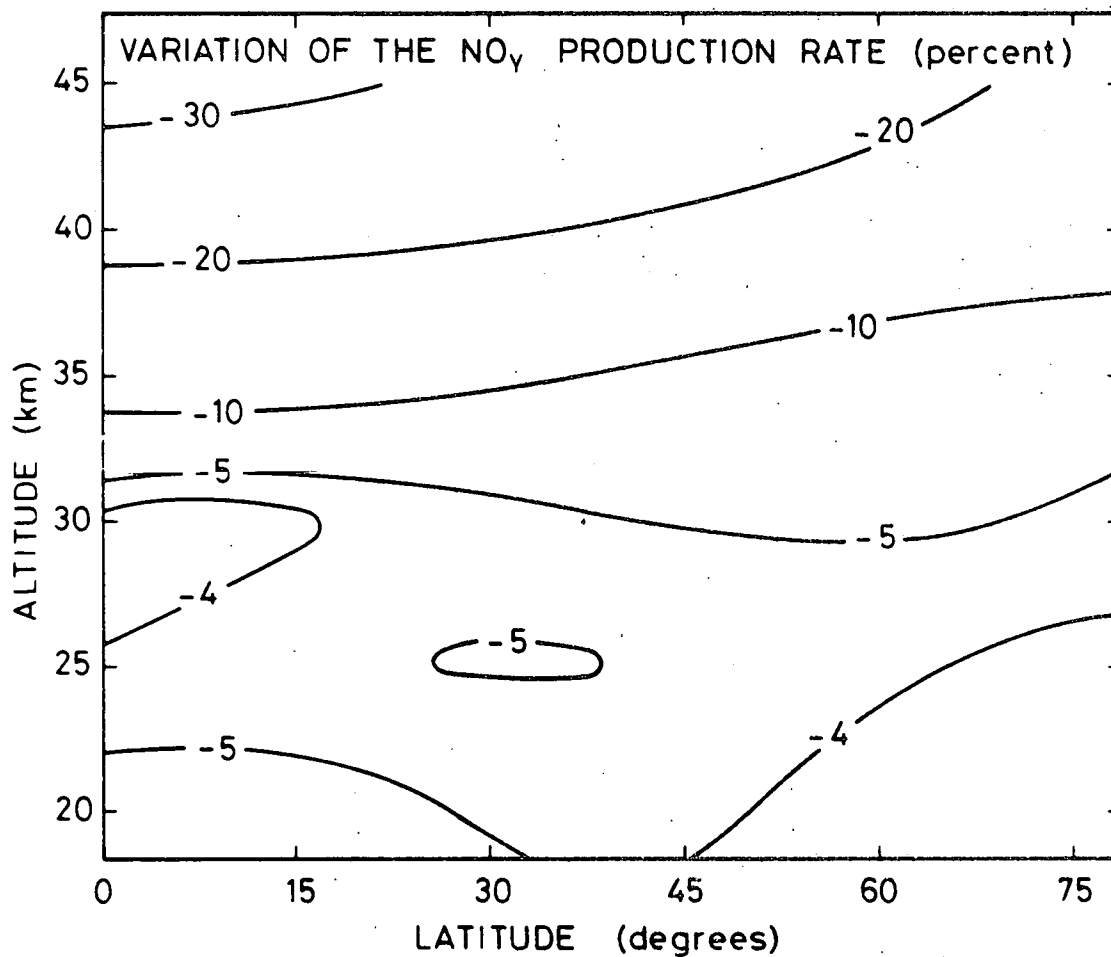


Fig. 16.- Meridional distribution of the change in the nitric oxide production rate for the UV variability from solar minimum to maximum (fig. 2). Temperature feedback taken into account.

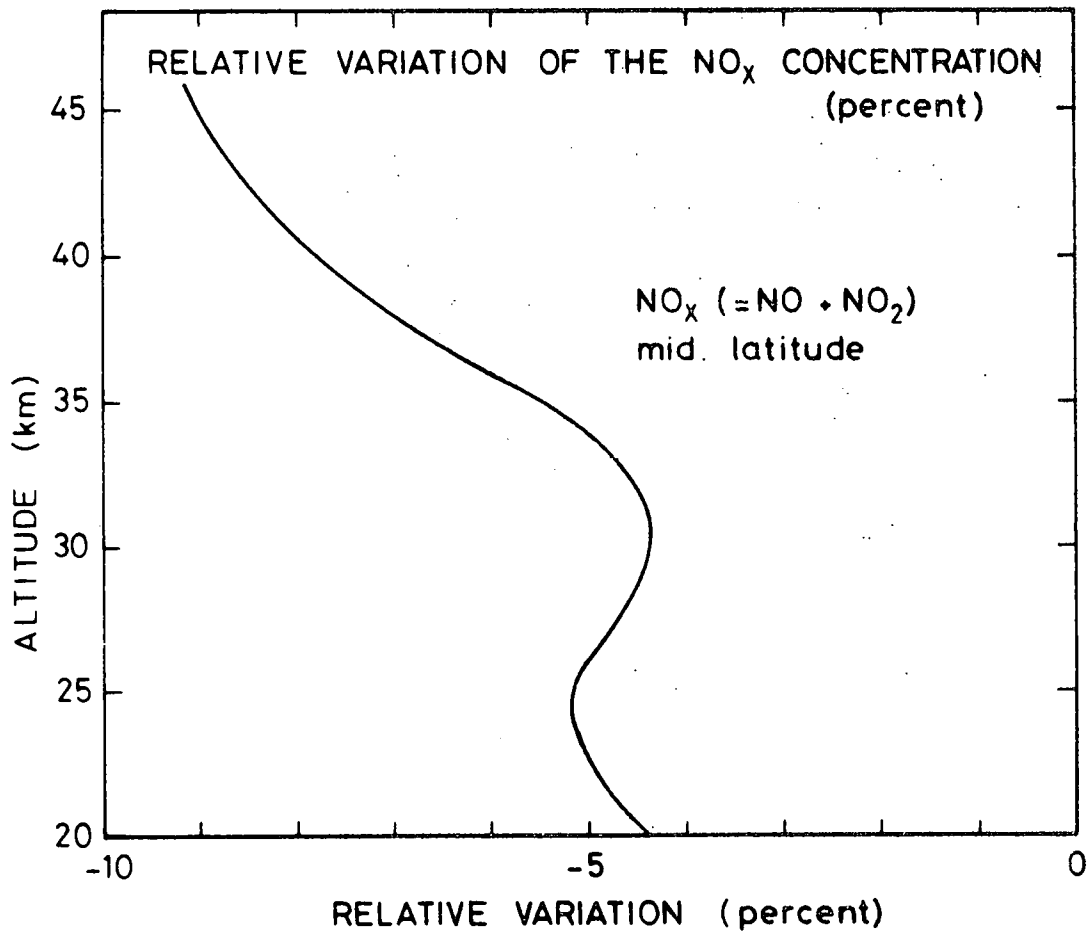


Fig. 17.- Vertical distribution of the relative change in the NO<sub>x</sub> (NO + NO<sub>2</sub>) concentration at 30 degrees latitude for the UV variability from solar minimum to solar maximum (fig. 2). Temperature feedback taken into account.

However, the best estimates of the ozone amount made between 1957 and 1975 (see e.g. the analysis of Angell and Korshover, 1973; 1976; 1978a) provide no unambiguous evidence that total ozone varies significantly with solar cycle. Dütsch (1979; personal communication) has reported such a possible correlation with a time lag of the order of 2 years but his analysis is based on the data from a single station, namely Arosa in Switzerland. Consequently, the solar flux variability suggested in this work seems to be more acceptable than the values proposed earlier and, with the data presently available, should even be considered as an upper limit. In fact if there is a long-term variability in the solar irradiance, it should appear in the behavior of more sensitive species such as  $N_2O$ . Therefore a monitoring of this gas in the upper stratosphere should give unambiguous information concerning the possible existence of solar flux variability. Finally long-term observation of the UV irradiance is required since the response of the stratosphere to anthropogenic perturbations cannot be carefully studied without considering the natural variability of the various trace species..

#### ACKNOWLEDGMENT

The authors are indebted to C. Nicolis for her collaboration in developing the thermal scheme used in this work. They also thank P. De Baets for his help in the numerical treatment of this problem.

## APPENDIX : DESCRIPTION OF THE IAS 2-D MODEL

### 1. Introduction

The IAS 2-D model has been constructed to investigate the structure of the natural atmosphere and to study the behavior of stratospheric minor constituents (Brasseur, 1978; Brasseur and Bertin, 1974; 1976; 1978). It can be run for several conditions, namely

1. in a steady state version with an oversimplified transport parameterization. This version has been used in the present work since it is not highly time consuming.
2. in a time-dependent version with a less detailed chemistry but a more elaborated transport representation.

### 2. Physical domain and equations

The physical domain of the model extends from the ground (0 km) to the stratopause (50 km) and from the North pole (+ 90°) to the South pole (- 90°). For each constituent  $i$  (or family or constituents - see below), one solves a continuity equation, namely ;

$$\begin{aligned} & [v] \frac{\partial n_i}{a \partial \varphi} + [w] \left\{ \frac{\partial [n_i]}{\partial z} + \frac{[n_i]}{H} \right\} \\ & + \frac{1}{a \cos \varphi} \frac{\partial}{\partial \varphi} [n_i^* v_i^*] \cos \varphi + \frac{\partial}{\partial z} [n_i^* w_i^*] = [P_i] - [L_i] \end{aligned} \quad (1)$$

where  $n_i$  is the concentration of species  $i$ ,  $v$  and  $w$  respectively the meridional and vertical wind component,  $H$  the atmospheric scale height,  $\varphi$  the latitude,  $z$  the altitude,  $a$  the Earth's radius,  $P_i$  and  $L_i$  respectively the production and the loss rates. The brackets refer to zonal mean variables and the stars to the deviations from this average.



The components of the wind related to the mean general circulation are prescribed as fixed parameters. The wave or eddy components are parameterized in the model using the generalized diffusion equation suggested by Demazure and Saïssac (1962) and Reed and German (1965) :

$$[n_i^* v_i^*] = - n(M) \left[ K_{yy} \frac{\partial [f_i]}{\partial \varphi} + K_{yz} \frac{\partial [f_i]}{\partial z} \right] \quad (2.a)$$

$$[n_i^* w_i^*] = - n(M) \left[ K_{zy} \frac{\partial [f_i]}{\partial \varphi} + K_{zz} \frac{\partial [f_i]}{\partial z} \right] \quad (2.b)$$

where  $f_i = n_i/n(M)$  is the volume mixing ratio and  $n(M)$  the total atmospheric concentration.

The transport parameters used in the model differ from one version to another. In the time dependent approach, the wind components are usually taken from Cunnold et al. (1975). The distribution of the exchange coefficients ( $K_{ij}$ ) are based on the shape of the profiles given by Gudiksen et al. (1968) and Luther (1973) but are adjusted by a "trial and error" method (Brasseur; 1980) to give the best agreement between the observed and calculated ozone distribution. In order to facilitate the determination of the K values, it is assumed that they can be expressed as a function of latitude ( ) alone multiplied by a function of height (z) alone (variable separation) :

$$K_{ij}(\varphi, z) = K_{ij}(\varphi, 20 \text{ km}) \times \gamma_{ij}(z) \quad (3)$$

Figure A-1 shows the result of this calibration.

In the steady state version of the model, oversimplified transport conditions are adopted. The mean circulation is not considered while the eddy diffusion components distribution are kept simple.  $K_{yy}$  and  $K_{zz}$  are constant in the whole domain and equal to  $10^{10} \text{ cm}^2 \text{ s}^{-1}$  and  $10^4 \text{ cm}^2 \text{ s}^{-1}$  respectively.  $K_{yz}$  is adjusted until the meridional distribution of

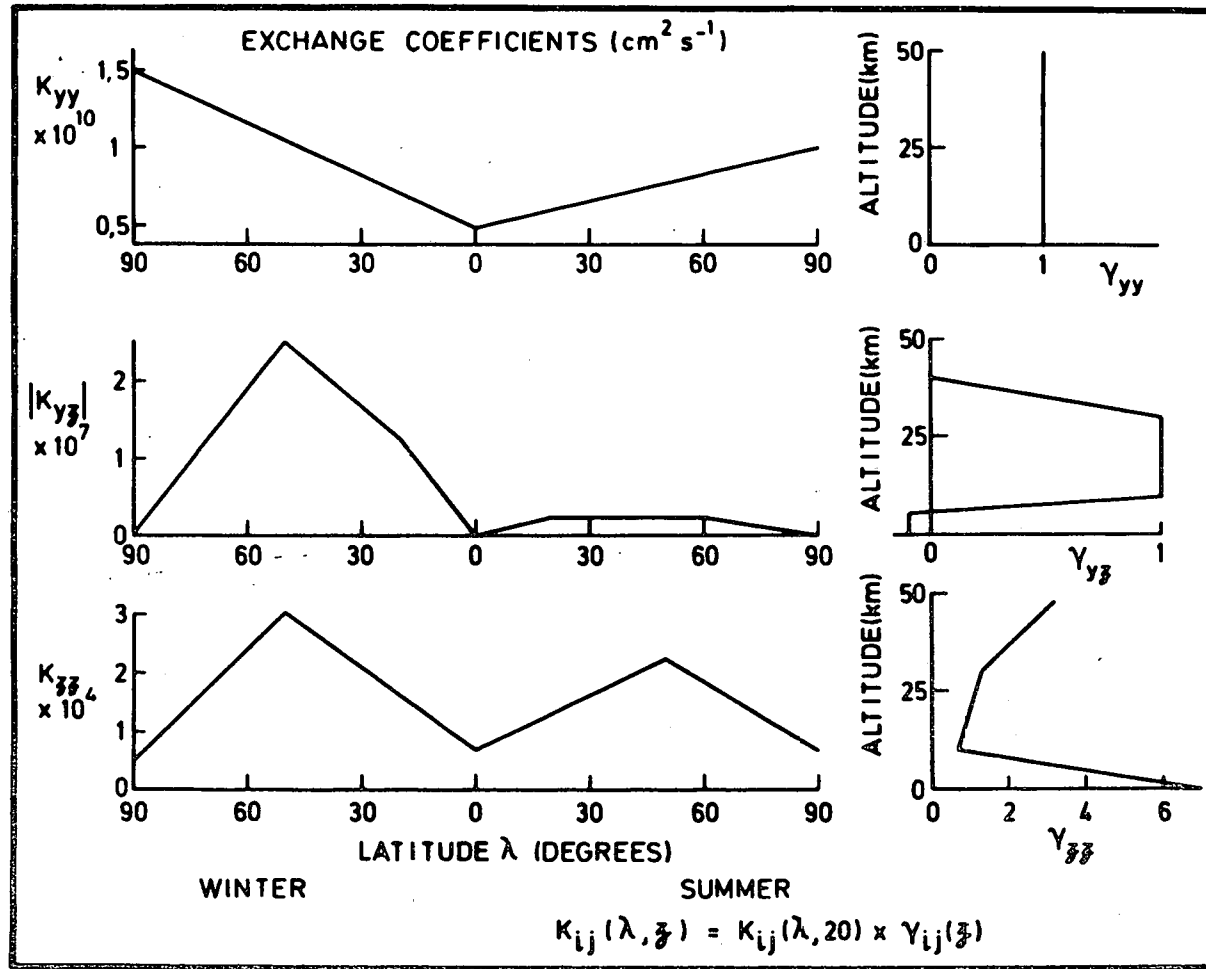


Fig. A-1 Distribution of the exchange coefficients versus latitude and altitude adopted after adjustment in the time dependent version of the model.

ozone becomes realistic (see figure A-2). It is interesting to note that such a elementary parametrization leads to distributions of chemical species which are in rather good agreement with the observation or with the results obtained when a more elaborated transport representation is adopted.

The meridional distribution of the temperature is derived from the energy equation

$$\begin{aligned}
 [v] \frac{\partial[\theta]}{a \partial \varphi} + [w] \frac{\partial[\theta]}{\partial z} + \frac{1}{a \cos \varphi} \frac{\partial}{\partial \lambda} ([v^* \theta^*] \cos \varphi) \\
 + \frac{\partial}{\partial z} [w^* \theta^*] - \frac{[w^* \theta^*]}{H} = \frac{[Q]}{\rho C_p} \left( \frac{p_0}{p} \right)^\kappa
 \end{aligned}$$

where

$$\theta = T \left( \frac{p_0}{p} \right)^\kappa$$

is the potential temperature,  $p$  the atmospheric pressure,  $p_0 = 1000$  mb,  $\kappa$  the factor  $R/C_p$ ,  $R$  the perfect gas constant,  $C_p$  the specific heat at constant pressure and  $\rho$  the atmospheric mass density.  $Q$  is the net heating rate which is related to the UV absorption or IR emission by chemical species.

Above 30 km, the heating due to the absorption of UV radiation by the Hartley and Huggins bands of ozone is calculated explicitly while the infrared cooling related to the emission mainly by carbon dioxide ( $15 \mu\text{m}$ ) and by ozone ( $9.6 \mu\text{m}$ ) is parameterized by means of the empirical relation of Dickinson (1973) :

$$\begin{aligned}
 Q = n(O_3) \int_{\nu} \varepsilon_{\nu}(z, \chi) \sigma_{\nu} d\nu - \\
 [L_{\text{ref}}(z) + a(z) (T(y, z) - T_{\text{ref}}(z))]
 \end{aligned}$$

where  $n(O_3)$  is the local ozone concentration,  $\varepsilon_{\nu}$  the solar energy at the

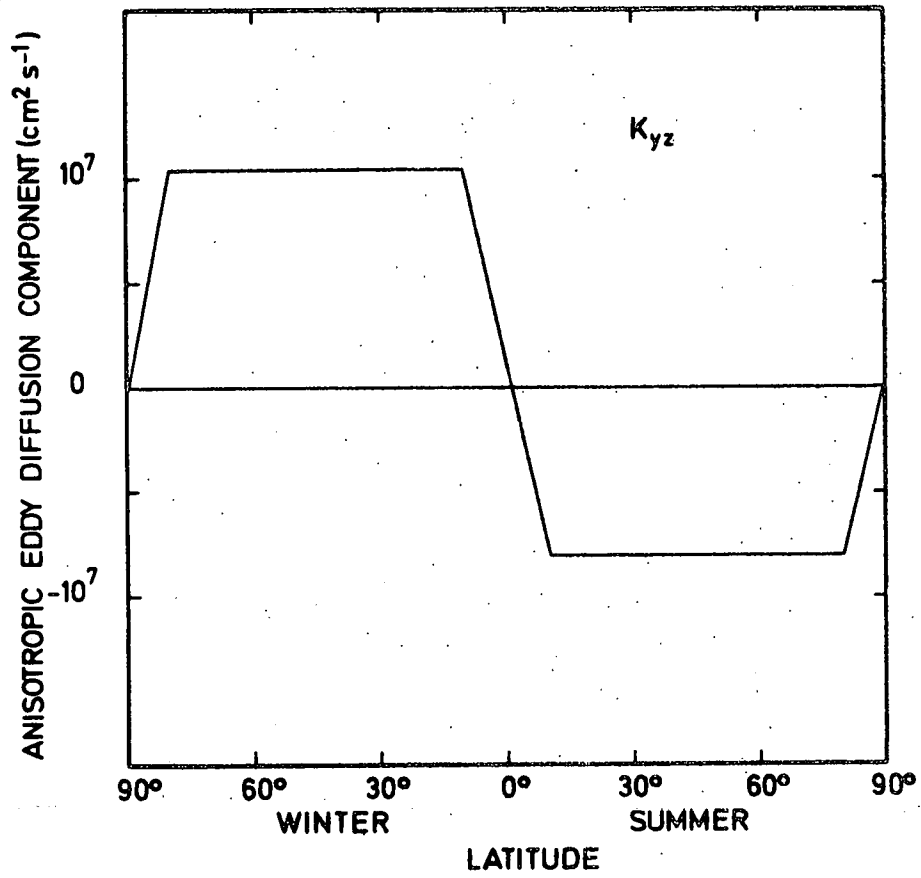


Fig. A-2 Latitudinal distribution of  $K_{yz}$  (absolute value) adopted below 25 km in the steady state model.

frequency  $\nu$ , altitude  $z$  and solar zenith angle  $\chi$ , and  $\sigma_{\nu}(\text{O}_3)$  the absorption cross section of ozone.  $L_{\text{ref}}(z)$  is the cooling rate calculated by Dickinson (1973) in a reference 1-D atmosphere with a temperature profile  $T_{\text{ref}}(z)$ .  $T(y, z)$  is the actual temperature at latitude  $y$  and altitude  $z$  and  $a(z)$  is a Newtonian cooling coefficient which is also determined as a function of the altitude by Dickinson (1973). In the lower stratosphere and in the troposphere where the heating by ozone becomes negligible, the effect of latent heat becomes significant. Therefore, below 20 km, the net heating rate is parameterized by the following expression suggested by Trenberth (1973)

$$\frac{Q}{\rho C_p} = h(z) [T^*(\varphi, z) - T(\varphi, z)]$$

where  $h(z)$  is a Newtonian cooling coefficient including boundary layer heating and latent heat release, and  $T^*(y, z)$  is an average equilibrium temperature obtained from data. Between 20 and 30 km a linear combination of both methods is used. The turbulent transport of heat is represented by :

$$[v^* \theta^*] = - \left\{ K_{yy} \frac{\partial[\theta]}{a \partial \varphi} + K_{yz} \frac{\partial[\theta]}{\partial z} \right\}$$

$$[w^* \theta^*] = - \left\{ K_{zy} \frac{\partial[\theta]}{\partial \varphi} + K_{zz} \frac{\partial[\theta]}{\partial z} \right\}$$

The exchange coefficients for heat transport are of the same order of magnitude as the coefficients related to the transport of chemical species but have not always the same value.

### 3. Chemical species

The chemical and photochemical scheme used in the model (table IV and V) results from the analysis of stratospheric reactions made by several authors (e.g. Nicolet, 1975) or working groups (e.g. NASA, 1977).

TABLE IV.- Principal chemical reactions in the stratosphere and their rate constants

Reaction	Rate constant (cm <sup>3</sup> s <sup>-1</sup> )	Reference
$O + O + M \rightarrow O_2 + M$	$k_1 = 4.7 \times 10^{-33} \left(\frac{300}{T}\right)^2 n(M)$	Nicolet (1975)
$O + O_2 + M \rightarrow O_3 + M$	$k_2 = 1.1 \times 10^{-34} e^{510/T} n(M)$	Hampson and Garvin (1978)
$O + O_3 \rightarrow O_2 + O_2$	$k_3 = 1.9 \times 10^{-11} e^{-2300/T}$	Hampson (1973)
$O(^1D) + N_2 \rightarrow O(^3P) + N_2$	$k_4 = 2.0 \times 10^{-11} e^{107/T}$	Davidson <u>et al.</u> (1977)
$O(^1D) + O_2 \rightarrow O(^3P) + O_2$	$k_5 = 2.9 \times 10^{-11} e^{67/T}$	Davidson <u>et al.</u> (1977)
$H + O_2 + M \rightarrow HO_2 + M$	$a_1 = 2.1 \times 10^{-32} e^{290/T} n(M)$	Wong and Davis (1974)
$H + O_3 \rightarrow O_2 + OH^+_{v=9}$	$a_2 = 1.0 \times 10^{-10} e^{-516/T}$	Clyne and Monkhouse (1977)
$OH + O \rightarrow H + O_2$	$a_5 = 4.0 \times 10^{-11}$	Working value, cf. Wilson (1972)
$OH + O_3 \rightarrow HO_2 + O_2$	$a_6 = 1.5 \times 10^{-12} e^{-1000/T}$	NASA (1977)
$HO_2 + O_3 \rightarrow OH + 2O_2$	$a_{6b} = 1.4 \times 10^{-14} e^{-580/T}$	Zahniser and Howard (1978)
$HO_2 + O \rightarrow O_2 + OH^+_{v=6}$	$a_7 = 3.5 \times 10^{-11}$	Burrows, Harris and Thrush (1977)
$O(^3P) + NO_2 \rightarrow NO + O_2$	$b_3 = 9.1 \times 10^{-12}$	Davis, Herron and Huie (1973)
$O_3 + NO \rightarrow NO_2 + O_2$	$b_4 = 2.1 \times 10^{-12} e^{-1450/T}$	NASA (1977)
$N(^4S) + NO \rightarrow N_2 + O$	$b_6 = 8.2 \times 10^{-11} e^{-410/T}$	Clyne and Mc Dermid (1975)
$N(^4S) + O_2 \rightarrow NO + O$	$b_7 = 5.5 \times 10^{-12} e^{-3200/T}$	Becker <u>et al.</u> (1969)

TABLE IV.- Principal chemical reactions in the stratosphere and their rate constants

Reaction	Rate constant (cm <sup>3</sup> s <sup>-1</sup> )	Reference
$\text{NO}_2 + \text{O}_3 \rightarrow \text{NO}_3 + \text{O}_2$	$b_9 = 1.2 \times 10^{-13} e^{-2450/T}$	NASA (1977)
$\text{NO}_3 + \text{NO}_2 + \text{M} \rightarrow \text{N}_2\text{O}_5 + \text{M}$	$b_{12} = 2.8 \times 10^{-30} n(\text{M})$ $= 3.8 \times 10^{-12}$ (limiting value)	Baulch <u>et al.</u> (1973)
$\text{NO}_2 + \text{OH} + \text{M} \rightarrow \text{HNO}_3 + \text{M}$	$b_{22}$ see below	NASA (1977)
$\text{HNO}_3 + \text{OH} \rightarrow \text{H}_2\text{O} + \text{NO}_3$	$b_{27} = 9 \times 10^{-14}$	Margitan <u>et al.</u> (1975)
$\text{N}_2\text{O}_5 + \text{M} \rightarrow \text{NO}_3 + \text{NO}_2 + \text{M}$	$b_{32} = 2.2 \times 10^{-5} e^{-9700/T}$ $= 5.7 \times 10^{14} e^{-10600/T}$ (limiting value) of $b_{32} n(\text{M})$	Baulch et al (1973)
$\text{N}_2\text{O} + \text{O}(^1\text{D}) \rightarrow \text{N}_2 + \text{O}_2$	$b_{38} = 5.5 \times 10^{-11}$	Davidson <u>et al</u> (1977)
$\text{N}_2\text{O} + \text{O}(^1\text{D}) \rightarrow 2 \text{NO}$	$b_{39} = 5.5 \times 10^{-11}$	Cvetanovic (1974)
$\text{HO}_2 + \text{NO}_2 + \text{M} \rightarrow \text{HO}_2\text{NO}_2 + \text{M}$	$b_{23} = 7.5 \times 10^{-33} e^{+\frac{1000}{T}}$ $\times \frac{1}{1 + 4.9 \times 10^{-12} [n(\text{M})]^{0.61}}$	Howard (1978)
$\text{OH} + \text{OH} \rightarrow \text{H}_2\text{O} + \text{O}$	$a_{16} = 1 \times 10^{-11} e^{-550/T}$	Baulch <u>et al.</u> (1972)
$\text{OH} + \text{HO}_2 \rightarrow \text{H}_2\text{O} + \text{O}_2$	$a_{17} = 3 \times 10^{-11}$	NASA (1977)

TABLE IV.- Principal chemical reactions in the stratosphere and their rate constants

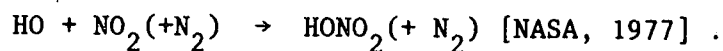
Reaction	Rate constant (cm <sup>3</sup> s <sup>-1</sup> )	Reference
H + HO <sub>2</sub> → OH + OH	a <sub>23a</sub> = 4.2 × 10 <sup>-10</sup> e <sup>-950/T</sup>	Baulch <u>et al.</u> (1972)
H + HO <sub>2</sub> → H <sub>2</sub> O <sub>2</sub>	a <sub>23b</sub> = 4.2 × 10 <sup>-11</sup> e <sup>-350/T</sup>	Baulch <u>et al.</u> (1972)
H + HO <sub>2</sub> → H <sub>2</sub> O + O	a <sub>23c</sub> = 8.3 × 10 <sup>-11</sup> e <sup>-500/T</sup>	Lloyd (1974)
H <sub>2</sub> + O( <sup>3</sup> P) → OH + H	a <sub>24</sub> = 8.8 × 10 <sup>-12</sup> e <sup>-4200/T</sup>	Dubnsky and McKenny (1975)
HO <sub>2</sub> + NO → NO <sub>2</sub> + OH	a <sub>26</sub> ≡ b <sub>29</sub> = 3.3 × 10 <sup>-12</sup> e <sup>254/T</sup>	
HO <sub>2</sub> + HO <sub>2</sub> → H <sub>2</sub> O <sub>2</sub> + O <sub>2</sub>	a <sub>27</sub> = 2.5 × 10 <sup>-12</sup>	Hamilton and Lii (1977)
OH + CO → CO <sub>2</sub> + H	a <sub>36</sub> = 1.4 × 10 <sup>-13</sup>	NASA (1977)
O( <sup>1</sup> D) + H <sub>2</sub> O → OH + OH	a <sub>1</sub> <sup>*</sup> = 2.3 × 10 <sup>-10</sup>	Davison <u>et al</u> (1977)
O( <sup>1</sup> D) + CH <sub>4</sub> → CH <sub>3</sub> + OH	a <sub>2</sub> <sup>*</sup> = 1.4 × 10 <sup>-10</sup>	Davidson <u>et al</u> (1977)
O( <sup>1</sup> D) + H <sub>2</sub> → OH + H	a <sub>3</sub> <sup>*</sup> = 1.0 × 10 <sup>-10</sup>	Davidson <u>et al</u> (1977)
CH <sub>4</sub> + OH → CH <sub>3</sub> + H <sub>2</sub> O	c <sub>2</sub> = 2.36 × 10 <sup>-12</sup> e <sup>-1710/T</sup>	Davis <u>et al</u> (1974)
CH <sub>3</sub> O <sub>2</sub> + NO → CH <sub>3</sub> O + NO <sub>2</sub>	c <sub>5</sub> = 3.3 × 10 <sup>-12</sup> e <sup>-500/T</sup>	Demerjian <u>et al.</u> (1974)
CH <sub>3</sub> Cl + OH → CH <sub>2</sub> Cl + H <sub>2</sub> O	d <sub>1</sub> = 2.2 × 10 <sup>-12</sup> e <sup>-1142/T</sup>	NASA (1977)
Cl + O <sub>3</sub> → ClO + O <sub>2</sub>	d <sub>2</sub> = 2.7 × 10 <sup>-11</sup> e <sup>-257/T</sup>	Watson (1977)
ClO + O → Cl + O <sub>2</sub>	d <sub>3</sub> = 7.7 × 10 <sup>-11</sup> e <sup>-130/T</sup>	NASA (1977)



TABLE IV.- Principal chemical reactions in the stratosphere and their rate constants

Reaction	Rate constant (cm <sup>3</sup> s <sup>-1</sup> )	Reference
ClO + NO → Cl + NO <sub>2</sub>	$d_4 = 1.0 \times 10^{-11} e^{+200/T}$	NASA (1977)
Cl + CH <sub>4</sub> → HCl + CH <sub>3</sub>	$d_5 = 7.3 \times 10^{-12} e^{-1260/T}$	Watson (1977)
Cl + HO <sub>2</sub> → HCl + O <sub>2</sub>	$d_7 = 3 \times 10^{-11}$	Leu and DeMore (1976)
HCl + OH → Cl + H <sub>2</sub> O	$d_{11} = 3 \times 10^{-12} e^{-425/T}$	Watson (1977)
ClO + NO <sub>2</sub> + M → ClONO <sub>2</sub> + M	$d_{22} = \frac{3.3 \times 10^{-23} T^{-3,34} n(M)}{1 + 8.7 \times 10^{-9} T^{-0,6} [n(M)]^{0,5}}$	Zahniser <u>et al.</u> (1977)
ClONO <sub>2</sub> + O → products	$d_{32} = 3 \times 10^{-12} e^{-808/T}$	NASA (1977)
ClO + HO <sub>2</sub> → HOCl + O <sub>2</sub>	$d_{35} = 4.5 \times 10^{-12}$	Howard (1978)

TABLE IV bis Parameters for an Analytical Expression for the Second-Order Rate Constant of the Reaction



$$\log (b_{22}) = - AT/(B+T) - 0.5 \log_{10} (T/280)$$

$$A = A_1 + A_2Z + A_3Z^2 + A_4Z^3$$

$$B = B_1 + B_2Z + B_3Z^2$$

$$A_1 = 31.62273$$

$$B_1 = - 327.372$$

$$A_2 = - 0.258304$$

$$B_2 = 44.5586$$

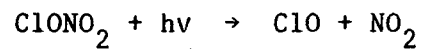
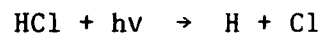
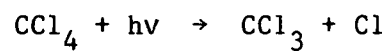
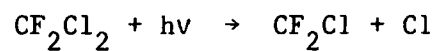
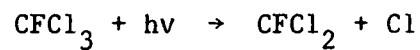
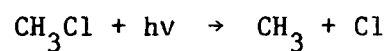
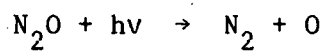
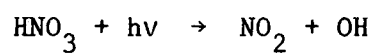
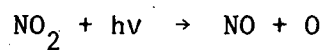
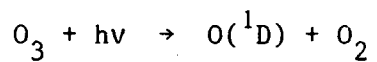
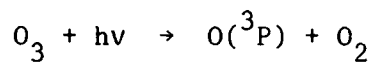
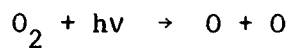
$$A_3 = - 0.0889287$$

$$B_3 = - 1.38092$$

$$A_4 = 2.520173 \times 10^{-3}$$

where  $Z = \log_{10}[\text{N}_2]$  and is applicable only for the range  $200 < T/K < 350$  and  $16.3 < \log_{10}([\text{N}_2]/\text{molecule cm}^{-3}) < 19.5$ , with an estimated reliability in  $\log k$  of  $\pm 0.10$  (reliability analogous to  $1 \sigma$ ). Air is approximately 6 percent less efficient than nitrogen as a third body (i.e. the expression above may be used with  $[\text{Air}] = 0.94 [\text{N}_2]$ ).

TABLE V.- Principal photochemical reactions in the stratosphere.



In order to avoid numerical instability problems due to the stiffness of the system and to facilitate the use of large time-step when integrating the equations, species are grouped into families ( $O_x = O_3 + O(^3P) + O(^1D)$ ;  $NO_y = NO + NO_2 + HNO_3 + ClONO_2$ ;  $Cl_x = Cl + ClO + ClONO_2 + HCl$ ) and the continuity equations for these families are solved taking into account the transport effect and their external production and loss rates. The concentration of the individual species is then derived assuming local photochemical equilibrium between the constituents belonging to a specified family.

The average value of the solar flux over 24 hours  $\bar{q}$  is approximated by a two points discretisation as suggested by the MIT group. (Cunnold et al., 1975)

$$\bar{q} = \frac{\pi}{2\pi} [q(AH = \frac{\pi}{4}) + q(AH = \frac{3\pi}{4})]$$

where AH is the solar hour angle,  $\frac{\pi}{4}$  is the value of AH at sunset (or sunrise) and is given by

$$\cos \frac{\pi}{4} = - \operatorname{tg} \varphi \operatorname{tg} \delta$$

where  $\varphi$  is the latitude and  $\delta$  the solar declination. In the steady state version  $\delta$  is chosen to be equal to 10 degrees while in the time-dependent version  $\delta$  varies with season from - 23 degrees to + 23 degrees. In this case the flux is recomputed every 15 days.

#### 4. Boundary conditions

A zero horizontal flux of all trace species at the North (Winter) and the South (Summer) Pole is assumed so that the zonal symmetry around the terrestrial axis is respected. At the ground and at strato-pause level, a fixed concentration is specified. (Brasseur and Bertin,

1978). Most of the conditions at the upper boundary are based on the results provided by 1-D models which extend to higher altitudes. The lower condition related to chlorofluorocarbons is representative of a 1980 situation. It should be noted that this type of boundary condition implies that the chlorine flux into the model may be a function of the internal chemistry and therefore of the UV irradiance. However, since the tropospheric photodissociation of the chlorofluorocarbons is very weak, the change in the flux at ground level is small and the type of condition at ground level adopted here does not considerably influence the global picture of the results. Nevertheless further investigations of this question are required.

#### 5. Numerical treatment

The problem is treated numerically by approximating the space derivations by finite differences and by solving the system which is obtained using an alternating directions method (Paceman and Rachford, 1955). The grid spacing is 1 km in the vertical and 5 degrees ( $\sim 550$  km) in the horizontal. In the time-dependent version of the model, the time-step is usually chosen to be 1-5 days. The continuity equations related to the various species are treated successively and an iteration is performed in the steady state version until equilibrium conditions are reached.

#### 6. Selected results

Different simulations of the natural atmosphere have been undertaken with the various versions of the model. A typical evolution of total ozone at various latitudes is given in fig. A-3 while fig. A-4a and A-4b represent the meridional distribution of  $O_3$  in March and December and fig. A-5 the similar results for nitric acid in December. Fig. A-6 shows the distribution of the ozone concentration obtained with the steady state version of the model and fig. A-7 and A-8 the similar results for  $CFCl_3$  and HCl.

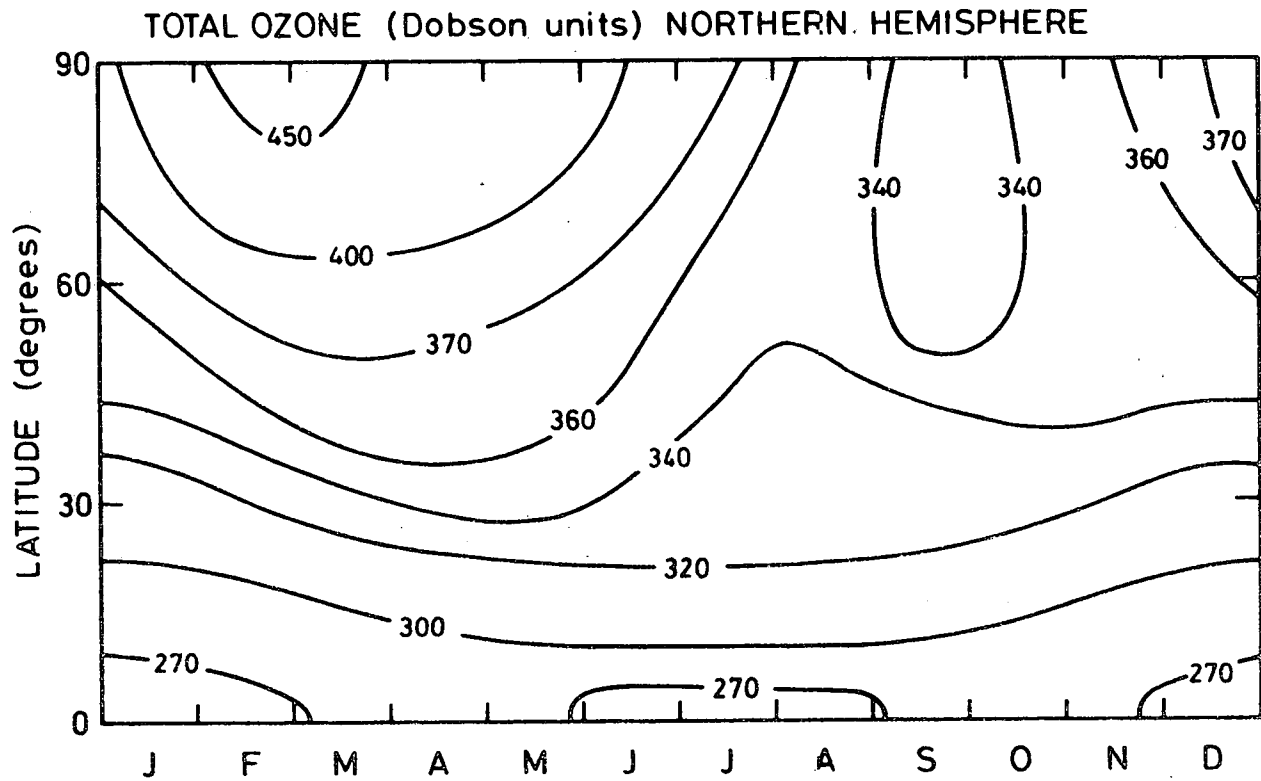


Fig. A-3 Predicted distribution of total ozone as a function of month and latitude.

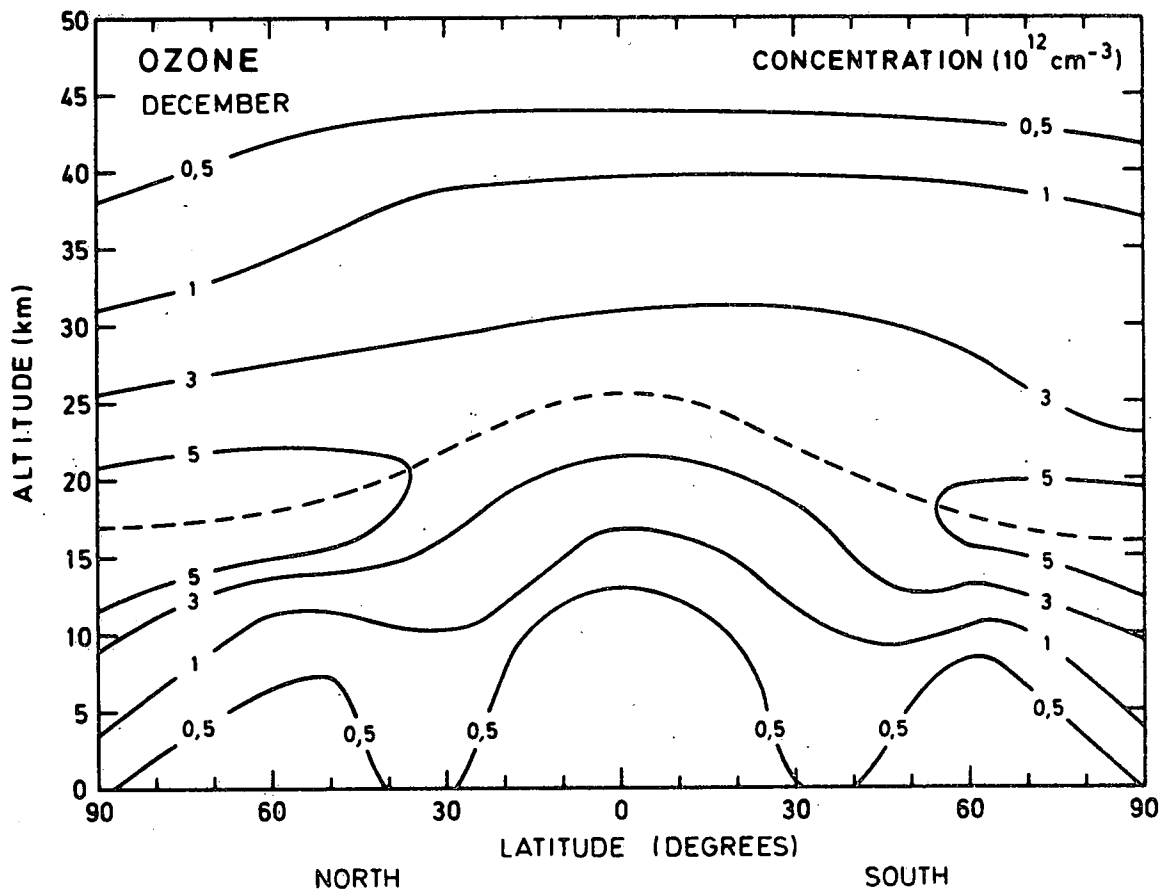
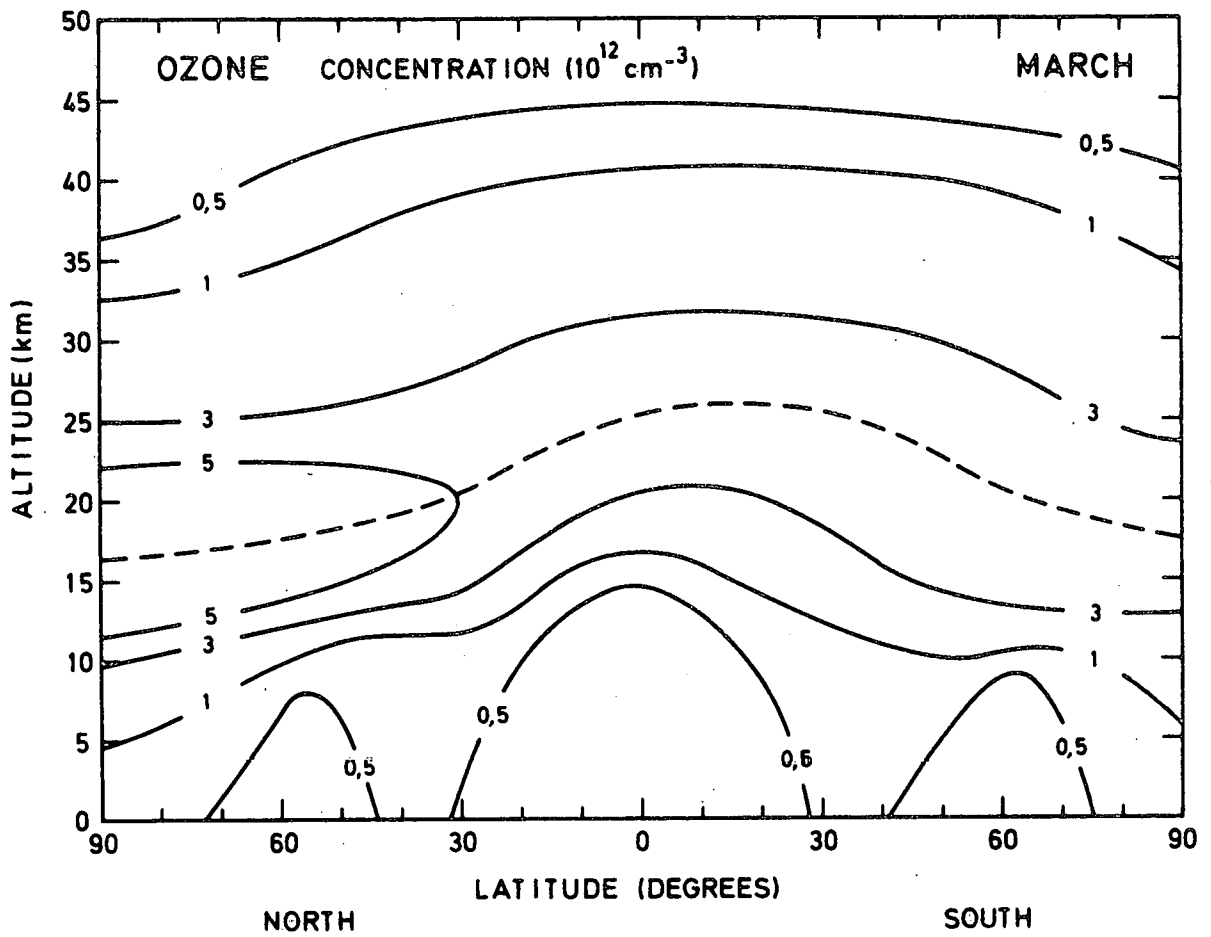


Fig. A-4 Meridional cross-section of the ozone concentration in March and December.

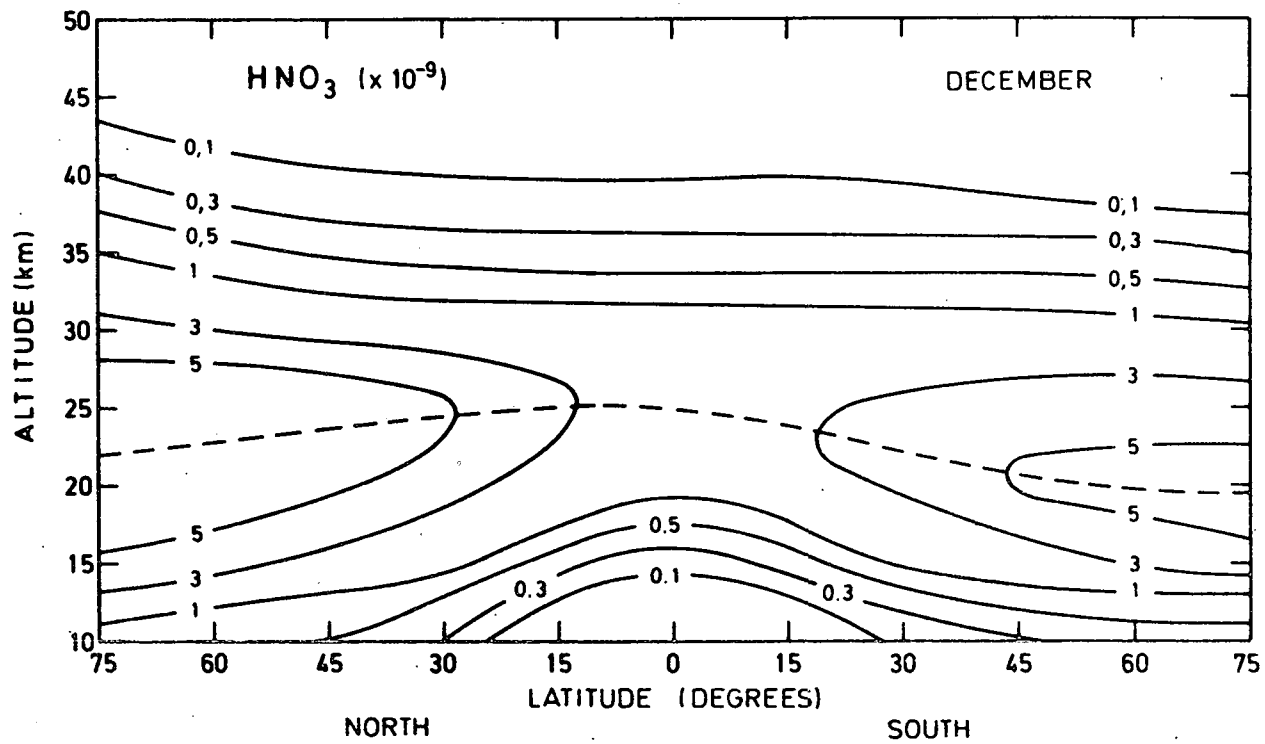


Fig. A-5 Meridional cross-section of the nitric acid volume mixing ratio obtained with the time dependent version of the model.



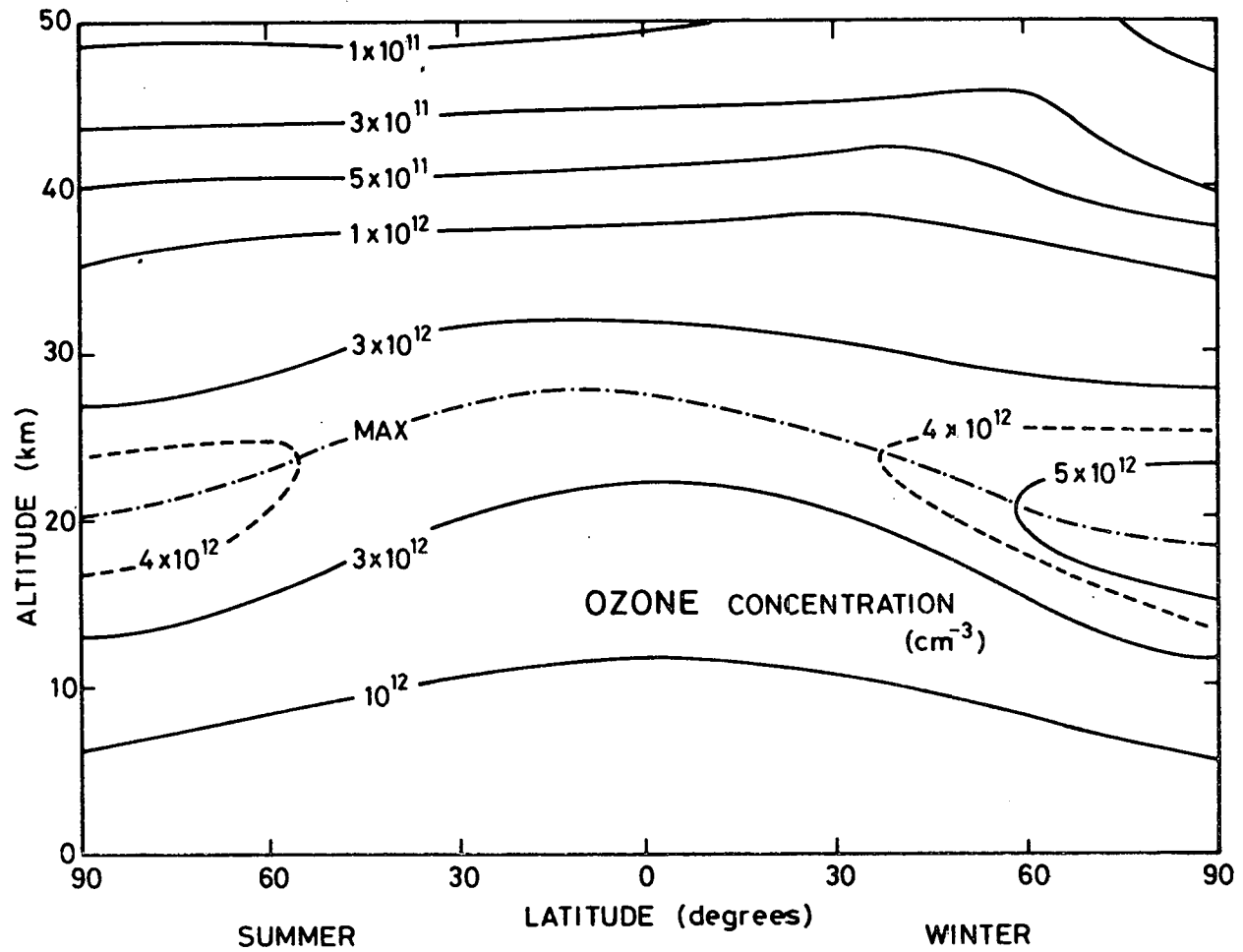


Fig. A-6 Meridional cross-section of the ozone concentration obtained with the steady-state version of the model.

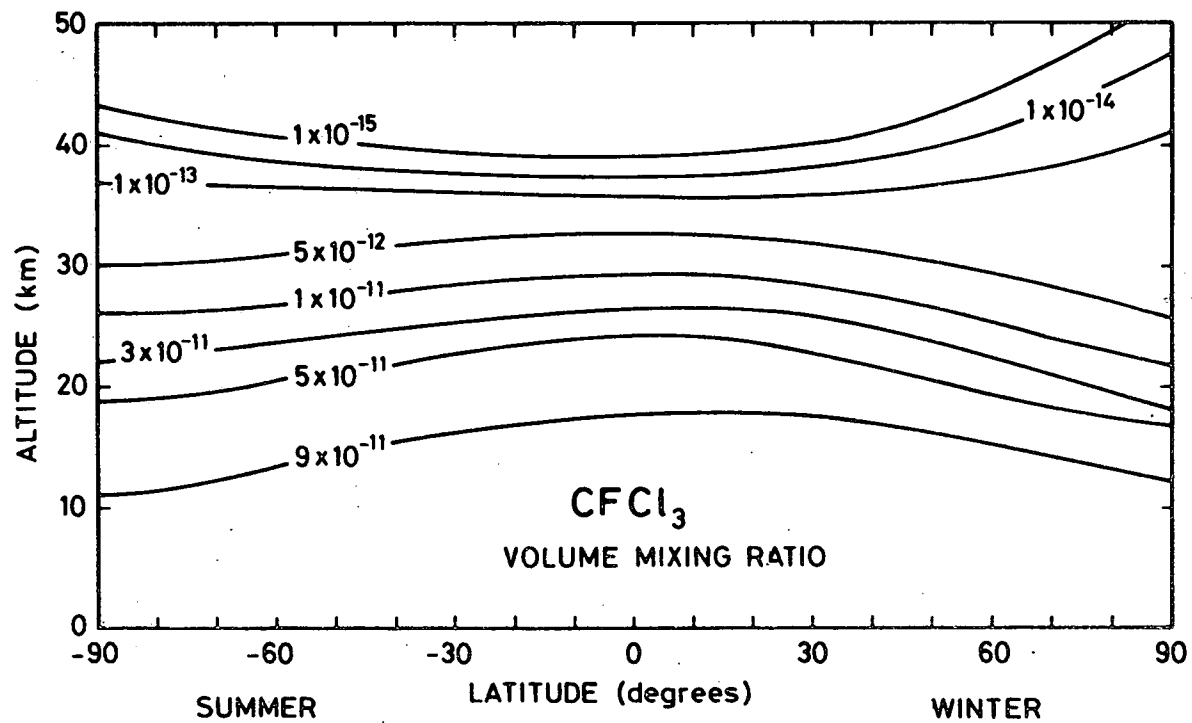


Fig. A-7 Meridional cross-section of the  $\text{CFCl}_3$  volume mixing ratio obtained with the steady state version of the model.

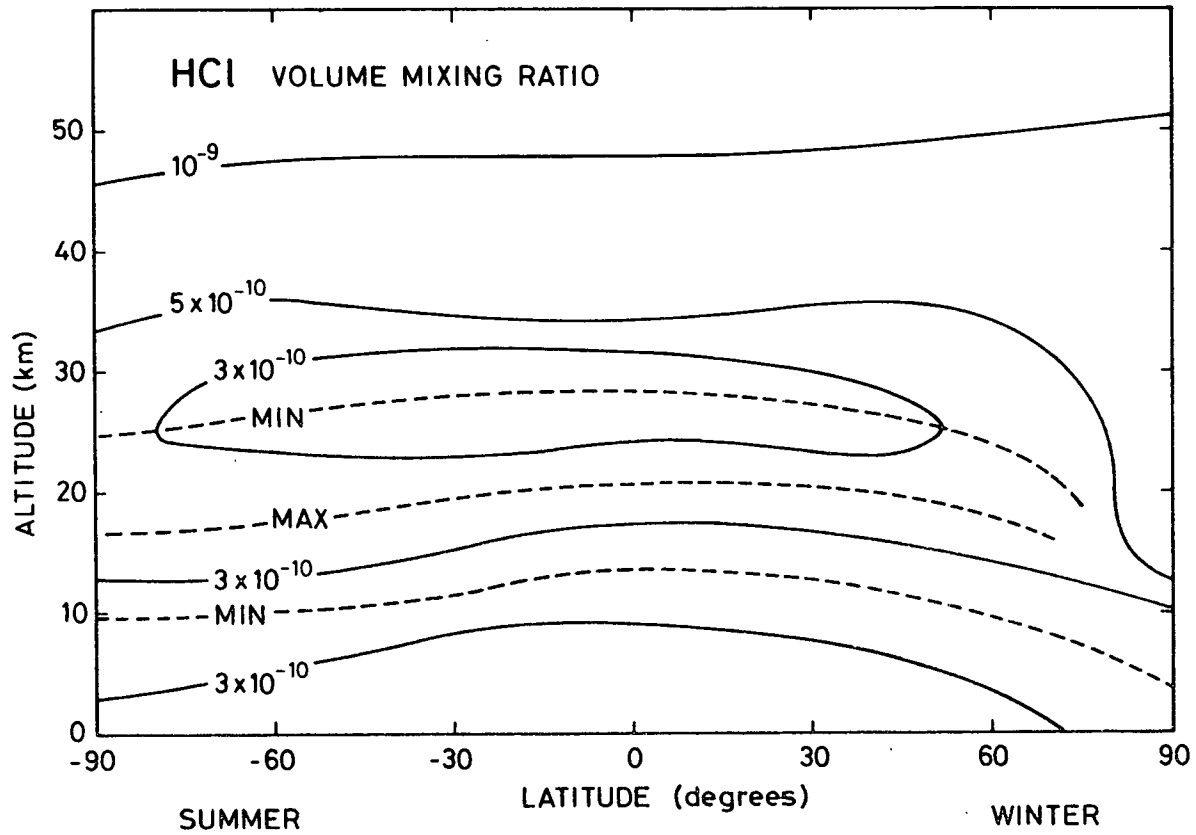
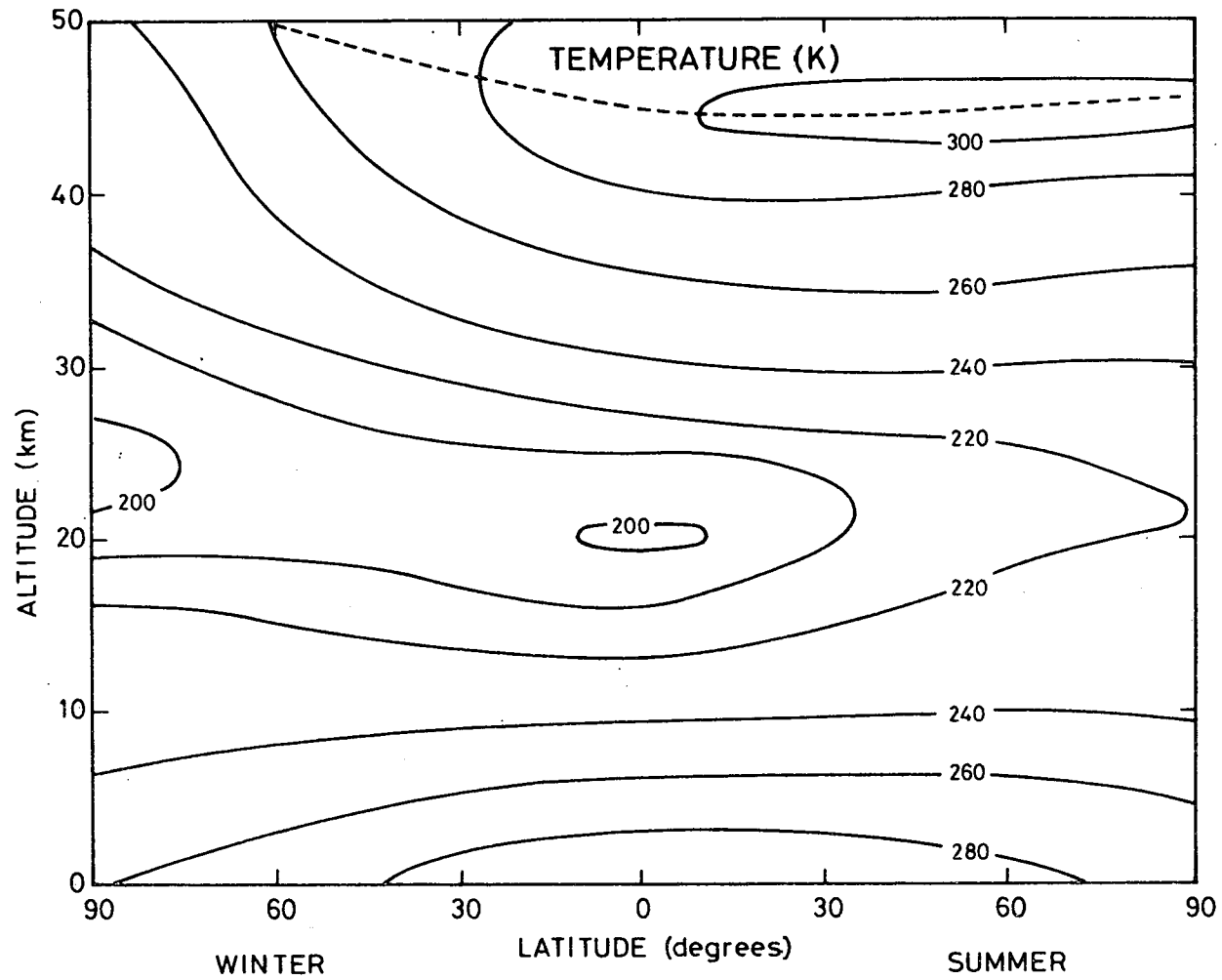


Fig. A-8 Meridional cross-section of the HCl volume mixing ratio obtained with the steady state version of the model.

RUN S 15



-74-

Fig. A-9 Meridional cross section of the temperature obtained with the steady state version of the model.

Finally, fig. A-9 depicts the meridional distribution of the temperature as computed with the steady state model.

## REFERENCES

- ANGELL, J.K., and J. KORSHOVER, Quasi-biennial and long-term fluctuations in total ozone, Month. Weath. Rev., 101, 426, 1973.
- ANGELL, J.K. and J. KORSHOVER, Global analysis of recent total ozone fluctuations, Month. Weath. Rev., 104, 63, 1976.
- ANGELL, J.K. and KORSHOVER, J., Global ozone variations : an update into 1976. Month. Weath. Rev., 106, 725, 1978a.
- ANGELL, J.K. and J. KORSHOVER, Recent rocket sonde - derived temperature variations in the Western Hemisphere, J. Atm. Sci., 35, 1958, 1978b.
- ARVESEN, J.C., R.N. GRIFFIN, and B.D. PEARSON, Jr., Determination of extraterrestrial solar spectral irradiance from a research aircraft, Appl. Optics, 8, 2215, 1969.
- BAULCH, D.L., D.D. DRYSDALE, D.G. HORNE and A.C. LLOYD, Evaluation Kinetic Data for high temperature reactions, vol. 1, Homogeneous Gas phase reactions of the H<sub>2</sub>-O<sub>2</sub> system, Butterworths, London, 1972.
- BAULCH, D.L., D.D. DRYSDALE, D.G. HORNE and A.C. LLOYD, Evaluated kinetic data for high temperature reactions, vol. 2, Homogeneous Gas phase reactions of the H<sub>2</sub>-N<sub>2</sub>-O<sub>2</sub> System, Butterworths, London, 1973.
- BECKER, K.H., W. GROTH and D. KLEY, The rate constant of the aeronomic reaction N + O<sub>2</sub>, Z. Naturforsch., A. 24, 1280, 1969.
- BRASSEUR, G., L'action des oxydes d'azote sur l'ozone dans la stratosphère, Aeronomica Acta A 173, 1976.
- BRASSEUR, G., Les modèles aéronomiques de la stratosphère. La Météorologie, Vie série, 15, 99, 1978.
- BRASSEUR, G., Un modèle bi-dimensionnel du comportement de l'ozone dans la stratosphère, Planet. Space Sci., 26, 139, 1978.
- BRASSEUR, G., On eddy diffusion coefficients, in Proceedings of the NATO Advanced Study Institute on Atmospheric Ozone, (ed. Aikin) p. 767, Portugal, 1979.

- BRASSEUR, G., to be published, 1980.
- BRASSEUR, G. and M. BERTIN, A theoretical two-dimensional model for minor constituents below 50 km, Second international conference on the environmental impact of Aerospace operations in the high atmosphere, Preprints, American Meteorological Society, 1974.
- BRASSEUR, G. and M. BERTIN, Distribution and circulation of stratospheric ozone in the meridional plane as given by a two-dimensional model, in Proceedings of the ozone symposium, Dresden, GDR, 1976.
- BRASSEUR G. and M. BERTIN, The action of chlorine on the ozone layer as given by a zonally averaged two-dimensional model, PAGEOPH, 117, 436, 1978.
- BRASSEUR, G. and M. NICOLET, Chemospheric processes of nitric oxide in the mesosphere and stratosphere, Planet. Space Sci., 21, 939, 1973.
- BROADFOOT, A.L., The solar spectrum 2100 - 3200 A, Astrophys. J., 173, 681, 1972.
- BRUECKNER, G.E., J.D. BARTOE, O. KJEDSETH MOE and M.E. VAN HOOSIER, Absolute solar ultraviolet intensities and their variations with solar activity, The wavelength region 1750 - 2100 A., Astrophys. J., 209, 935, 1976.
- BURROWS, J.P., G.W. HARRIS and B.A. THRUSH, Rates of reaction of HO<sub>2</sub> with HO and O studied by Laser Magnetic Resonance, Nature, 267, 233, 1977.
- CALLIS, L.B. and J.E. NEALY, The effect of U.V. variability on stratospheric thermal structure and trace constituents, Space Research, XVIII, 95, 1978.
- CALLIS, L.B. and J.E. NEALY, Solar UV variability and its effect on stratospheric thermal structure and trace constituents, Geophys. Res. Lett., 5, 249, 1978.
- CALLIS, L.B., M. NATARAJAN and J.E. NEALY, Ozone and temperature trends associated with the 11-year solar cycle, Science, 204, 1303, 1979.

- CLYNE, M.A.A. and I.S. McDERMID, Mass spectrometric determinations of the rate elementary reactions of NO and NO<sub>2</sub> with ground state N<sup>4</sup>S atoms, J. Chem. Soc. Faraday Trans., I, 71, 2189, 1975.
- CLYNE, M.A.A. and P.B. MONKHOUSE, Atomic resonance fluorescence for rate constants of rapid bimolecular reactions; H + NO<sub>2</sub> and H + O<sub>3</sub>, J. Chem. Soc. - Faraday Trans., II 73, 198, 1977.
- CUNNOLD, D., F. ALYEA, N. PHILLIPS and R. PRINN, A Three-dimensional dynamical - chemical model of atmospheric ozone, J. Atm. Sci., 32, 170, 1975.
- CVETANOVIC, R.J., Excited state chemistry in the stratosphere, Can. J. Chem., 52, 1452, 1974.
- DAVIS, D.D., S. FISCHER, and R. SCHIFF, Flash photolysis - resonance fluorescence kinetics study : temperature dependence of the reaction OH + CO → CO<sub>2</sub> + H and OH + CH<sub>4</sub> → H<sub>2</sub>O + CH<sub>3</sub>, J. Chem. Phys., 61, 2213, 1973.
- DAVIS, D.D., J.T. HERRON and R.H. HUIE, Absolute rate constants for the reaction O(<sup>3</sup>P) + NO<sub>2</sub> → NO + O<sub>2</sub> over the temperature range 230-339°K, J. Chem. Phys., 58, 530, 1973.
- DAVIDSON, J.A., H.I. SCHIFF, G.E. STREIT, J.R. McAFEE, A.L. SCHMELTEKOPF and C.J. HOWARD, Temperature dependence of O(<sup>1</sup>D) rate constants for reactions with N<sub>2</sub>O, H<sub>2</sub>, CH<sub>4</sub>, HCl and NH<sub>3</sub>, J. Chem. Phys., 67, 5021, 1977.
- DELABOUDINIÈRE, J.P., R.F. DONNELLY, H.E. HINTEREGGER, G. SCHMIDTKE and P.C. SIMON, Intercomparison/compilation of relevant solar flux data related to aeronomy, COSPAR -Technique Manual Series - Manual No 7, 1978.
- DEMAZURE, M. and J. SAISSAC, Généralisation de l'équation classique de diffusion, Note de l'Etablissement d'Etudes et de Recherches Météorologiques, No. 115, Paris 1962
- DEMERJIAN, K.L., J.A. KERR and J.C. CALVERT, The mechanism of photochemical smog formation, Adv. Environ. Sci. Technol., 4, 1, 1974.



- DICKISON, R.E., Method of parametrization for infrared cooling between altitudes of 30 and 70 km, J. Geophys. Res., 78, 4451, 1973.
- DUBINSKY, R.N. and D.J. MCKENNEY, Determination of the rate constant of the  $O + H_2 \rightarrow OH + H$  reaction using atomic oxygen resonance fluorescence and the air afterglow techniques, Can. J. Chem., 53, 3531, 1975.
- FREDERICK, J.E., Chemical response of the middle atmosphere to changes in the ultraviolet solar flux, Planet. Space Sci., 25, 1, 1977.
- GUDI KSEN, P.H., A.W. FAIRHALL and R.J. REED, Roles of mean meridional circulation and eddy diffusion in the transport of trace substances in the lower stratosphere, J. Geophys. Res., 73, 4461, 1968.
- HAMILTON, E.J. and R.R. LII, The dependence on  $H_2O$  and on  $NH_3$  of the kinetics of the self reaction of  $HO_2$  in the gas-phase formation of  $HO_2 \cdot H_2O$  and  $HO_2 \cdot NH_3$  complexes, Int. J. Chem. Kinet., 9, 875, 1977.
- HAMPSON, R.F., Survey of photochemical and rate data for twenty-eight reactions of interest in atmospheric chemistry. J. Phys. Chem., 2, 267, 1973.
- HAMPSON, R.F. and D. GARVIN, Reaction rate and photochemical data for atmospheric chemistry - 1977, National Bureau of Standards, Special publication, 513, 1978.
- HEATH, D.F., Space observations of the variability of solar irradiance in the near and far ultraviolet, J. Geophys. Res., 78, 2779, 1973.
- HEATH, D.F., Spatial and temporal variability of ozone as seen from space, in Proceedings of the NATO Advanced Study Institute on Atmospheric Ozone, (ed. Aikin) p. 45, Portugal, 1979.
- HEATH, D.F. and M.P. THEKAEKARA, in The solar output and its variation (ed. White), p. 193, Colo. Ass. Univ. Press., Boulder, USA, 1977.

- HEROUX, L. and H.E. HINTEREGGER, Aeronomical reference spectrum for solar UV below 2000 Å, J. Geophys. Res., 83, 5305, 1978.
- HEROUX, L. and R.A. SWIRBALUS, Full-disk solar fluxes between 1230 and 1940 Å, J. Geophys. Res., 81, 436, 1976.
- HINTEREGGER, H.E., Representations of solar EUV fluxes for aeronomical applications, Space Research, XXI, to be published, 1980.
- HINTEREGGER, H.E., and L.M. CHAIKIN, EUV absorption analysis of thermospheric structure from AE-satellite observations, Space Research, XVII, 525, 1977.
- HOWARD, C.J., Recent developments in atmospheric HO<sub>2</sub> chemistry, WMO symposium on the geophysical aspects and consequences of changes in the composition of the stratosphere, Toronto, 1978.
- HUMPHREYS, W.J., Solar disturbances and terrestrial temperatures, Astrophys. J., 32(2), 97, 1910.
- KJELDSETH MOE, O., M.E. VAN HOOSIER, J.D.F. BARTOE and G.E. BRUECKNER, A spectral atlas of the sun between 1175 and 2100 Å, NRL Report 8056, 1977.
- KOSTKOWSKI, H.J., Spectral irradiance scale change, Opt. Rad. News, N.B.S., 3, 5, 1974.
- LEU, M.T. and W.B. DE MORE, Rate constants at 295 K for the reactions of atomic chlorine with H<sub>2</sub>O<sub>2</sub>, HO<sub>2</sub>, O<sub>3</sub>, CH<sub>4</sub> and HNO<sub>3</sub>, Chem. Phys. Lett., 41, 121, 1976.
- LLOYD, A.C., Evaluated and estimated kinetic data for phase reactions of the hydroperoxyl radical, Int. J. Chem. Kinet., 6, 169, 1974.
- LONDON, J. and S. OLTMANS, Further studies of ozone and sunspot, PAGEOPH, 106-108, 1302, 1973.
- LUTHER, F.M., Monthly mean values of eddy diffusion coefficients in the lower stratosphere, AIAA/AMS international conference on the environmental impact of aerospace operations in the high atmosphere, Denver, Colorado, 1973.

- MARGITAN, J.J., F. KAUFMAN and J.G. ANDERSON, Kinetics of the reaction  $\text{OH} + \text{HNO}_3 \rightarrow \text{H}_2\text{O} + \text{NO}_3$ , Int. J. Chem. Kinet., Symp. No. 1, 281, 1975.
- MOUNT, G.N., G.J. ROTTMAN and J.G. TIMOTHY, The Solar Spectral Irradiance 1200-2250 Å at Solar Maximum, J. Geophys. Res., 85, 4271, 1980.
- NASA, National Aeronautics and Space Administration, Chlorofluoromethanes and the stratosphere, NASA - Reference Publication 1010, 1977.
- NECKEL, H. and D. LABS, Improved Data of Solar Spectral Irradiance from 0.33 to 1.25 μm, Solar Physics, to be published, 1981.
- NICOLET, M., Aeronomic reactions of hydrogen and ozone, in Mesospheric Models and Related Experiments, (ed. Fiocco), p. 1, D. Reidel, Dordrecht, Netherlands, 1971.
- NICOLET, M., On the production of nitric oxide by cosmic rays in the mesosphere and stratosphere, Planet. Space Sci., 23, 637, 1975.
- NICOLET, M., Stratospheric ozone : an introduction to its study, Rev. Geophys. Sp. Phys., 13, 593, 1975.
- NICOLET, M. and W. PEETERMANS, The production of nitric oxide in the stratosphere by oxidation of nitrous oxide, Ann. Geophys., 28, 751, 1972.
- POLLACK, J.B., W.J. BORUCKI and O.B. TOON, Are solar spectral variations a drive for climatic change ?, Nature, 282, 606, 1979.
- PAETZOLD, H.K., The influence of solar activity on the stratospheric ozone layer, PAGEOPH, 106-108, 1308, 1973.
- QUIROZ, R.S., Stratospheric temperatures during solar cycle 20, J. Geophys. Res., 84, 2415, 1979.
- ROTTMAN, G.L., Disc values of the solar ultraviolet flux 1150 Å to 1850 Å, Trans. An. Geophys. Un., 56, 1157, 1974.
- PENNER, J.E. and J.S. CHANG, Possible variations in atmospheric ozone related to the eleven-year solar cycle, Geophys. Res. Lett., 5, 817, 1978.

- PENNER, J.E. and J.S. CHANG, The relation between atmospheric trace species variabilities and solar UV variability, J. Geophys. Res., to be published, 1980.
- PENNER, J.E. and F.M. LUTHER, Effect of temperature feedback and hydrostatic adjustment in a stratospheric model, J. Atm. Sci., to be published, 1980.
- PEACEMAN, D.W. and H.H. RACHFORD, Jr., The numerical solution of parabolic and elliptic differential equations, J. Soc. indust. appl. Math., 3, 28, 1955.
- REED, R.J. and K.E. GERMAN, A contribution to the problem of stratospheric diffusion by large-scale mixing, Month. Weath. Rev., 93, 313, 1965.
- RUDERMAN, M.A. and J.W. CHAMBERLAIN, Origin of the sunspot modulation of ozone : Its implications for stratospheric NO injection, Planet. Space Sci., 23, 247, 1975.
- RYCROFT, N.J. and A.G. THEOBALD, Estimates of the stratospheric temperature variation in response to changes of the flux of solar UV radiation, Space Research, XVIII, 99, 1978.
- SAMAIN, D. and P.C. SIMON, Solar flux determination in the spectral range 150-210 nm, Solar Physics, 49, 33, 1976.
- SCHMIDTKE, G., Today's knowledge of the solar EUV output and the future needs for more accurate measurements for aeronomy, Planet. Space Sci., 26, 347, 1978.
- SIMON, P.C., Balloon measurements of solar fluxes between 1960 A and 2300 A, in Proceedings of the third conference on the climatic impact assessment program (eds. Broderick and Hard), p. 137, DOT-TSC-OST-74-15, 1974.
- SIMON, P.C., Nouvelles mesures de l'ultraviolet solaire dans la stratosphère, Bull. Acad. Roy. Belgique, Cl. Sci., 61, 399, 1975.
- SIMON, P.C., Irradiation solar flux measurements between 120 and 400 nm. Current position and future needs, Planet. Space Sci., 26, 355, 1978.

- SIMON, P.C., Observation of the Solar Ultraviolet Radiation, in Proceedings of the NATO Advanced Study Institute on Atmospheric Ozone, (ed. Aikin) p.529, Portugal, 1979.
- SIMON, P.C., R. PASTIELS and D. NEVEJANS, to be published, 1980.
- SIMON, P.C., Solar irradiance between 120 and 400 nm and its variations, Solar Physics, to be published, 1981.
- TRENBERTH, K.E., Global model of the General circulation of the atmosphere below 75 kilometers with an annual heating cycle, Month. Weath. Rev., 101, 287, 1973.
- VIDAL-MADJAR, A., Evolution of the solar Lyman alpha flux during four consecutive years, Solar Physics, 40, 69, 1975.
- WARNECK, P., Cosmic radiation as a source of odd nitrogen in the stratosphere, J. Geophys. Res., 77, 6589, 1972.
- WATSON, R.T., Rate constants for reactions of  $\text{ClO}_x$  of atmospheric interest, J. Phys. Chem. Ref. Data, 6, 871, 1977.
- WILLETT, H.C., The relationship of total atmospheric ozone to the sunspot cycle, J. Geophys. Res., 67, 661, 1962.
- WILSON, Wm. E., Jr., A critical Review of the gas-phase reaction kinetics of the hydroxyl radical, J. Phys. Chem. Ref. Data, 1, 535, 1972.
- WONG, W. and D.D. DAVIS, A flash photolysis-resonance fluorescence study of the reaction of atomic hydrogen with molecular oxygen :  $\text{H} + \text{O}_2 + \text{M} \rightarrow \text{HO}_2 + \text{M}$ , Int. J. Chem. Kinet., 6, 401, 1974.
- ZAHNISER, M.S., J.S. CHANG and F. KAUFMAN, Chlorine nitrate : Kinetics of formation by  $\text{ClO} + \text{NO}_2 + \text{M}$  and of reaction with OH, J. Chem. Phys., 67, 997, 1977.
- ZAHNISER, M.S. and C.J. HOWARD, WMO symposium on the geophysical aspects and consequences of changes in the composition of the stratosphere, Toronto, 1978.